TÉCNICO LISBOA

Further development of a rotary-wing preliminary design tool

Carlos Gallardo Borrego

Thesis to obtain the Master of Science Degree in

Aerospace Engineering

Supervisor: Professor Filipe Szolnoky Ramos Pinto Cunha

Examination Committee

Chairperson: Professor Afzal Suleman

Supervisor: Professor Filipe Szolnoky Ramos Pinto Cunha

Member of Committee: Professor Frederico José Prata Rente Reis Afonso

July 2022

I declare that this document is an original work of my own authorship and that it fulfills all the requirements of the Code of Conduct and Good Practices of the Universidade de Lisboa.

Acknowledgements

I would like to thank professor Filipe Szolnoky Cunha for the oportunity to work on this project, and for his outstanding guidance and dedication throughout the whole work.

A special thank you to my family and friends for their constant trust and support during this period.

Resumo

O objetivo deste trabalho é o melhoramento de uma ferramenta gratuita de código aberto dedicada à análise do desempenho de aeronaves de asa rotativa para ser utilizada em seu projeto preliminar.

Neste âmbito, foi adicionada à ferramenta a possibilidade de estudar helicópteros compostos, incluindo as duas configurações principais: helicóptero com asa e com hélice. A Teoria de Elementos de Pás e a Teoria de Perfis Finos foram usadas para modelar as asas e a Teoria de Elementos de Pás foi aplicada para analisar as hélices. As consequências da interação entre o rotor do helicóptero e os elementos compostos (asa e hélice) foram analisadas em detalhe.

Além da inclusão dessa nova funcionalidade na ferramenta, os cálculos de configurações simples de helicópteros também foram completados com a adição do efeito solo. Uma ferramenta diferente dedicada à análise de ciclocópteros foi ainda criada.

A validação dos resultados da ferramenta é feita e alguns estudos de caso são apresentados para garantir a confiabilidade das análises desenvolvidas.

Palavras chave: helicópteros compostos, Teoria de Elementos de Pás, Teoria de Perfis Finos, ciclocópteros, projeto preliminar.

Abstract

The objective of this work is to further develop an open-source tool dedicated to the analysis of the performance of rotary-wing aircrafts to be used for their preliminary design.

Under this scope, the possibility to study compound helicopters has been added to the tool, including the two main compound configurations: helicopter with a wing and with a propeller. Strip Theory and Thin Airfoil Theory have been used to model the wings and Blade Element Momentum Theory has been applied to analyse the propellers. The consequences of the interaction between the helicopter rotor and the compound elements (wing and propeller) have been analysed in detail.

Besides the inclusion of this new functionality in the tool, the calculations of simple helicopter configurations have also been completed with the addition of the ground effect. Moreover, a different tool dedicated to the analysis of cyclocopters has been created.

The validation and verification of the tools are done and some case studies are presented to ensure the reliability of the analysis developed.

Keywords: compound helicopters, Strip Theory, Thin Airfoil Theory, Blade Element Momentum Theory, cyclocopters, preliminary design.

Contents

List of Figures

List of Tables

List of Symbols

Greek symbols

α - Angle of attack [º]

α_{TPP} - Rotor tip path plane angle [º]

α_{ZL} - Zero lift angle of attack [º]

γ - Vortex strength [m/s]

Γ - Circulation [m^2/s]

Γ_0 - Circulation at the middle of the wing [m^2/s]

ϵ - Oswald efficiency factor

θ - Wing fixed incidence angle [º]

θ_0 - Coordinate in polar system where the wake starts hitting the wing [º]

θ_{traj} - Trajectory angle [º]

θ_{twist} - Twist angle [º]

ϕ - Inflow velocity angle [º]

ρ - Density [kg/m^3]

σ - Rotor solidity

χ - Wake angle [º]

ω - Rotation speed [rpm]

Roman symbols

a - Axial induction factor

a' - Radial induction factor

A - Area [m^2]

A_0, A_1 - Thin Airfoil Theory coefficients

A_f - Flat plate area [m^2]

AR - Wing aspect ratio

b - Wingspan [m]

c - Chord [m]

C_d - Drag coefficient

c_{inside} - Coordinate in x-axis where the wake starts hitting the wing [m]

C_l - Lift coefficient

$\bar{C_L}$ - Wing mean lift coefficient

C_n - Normal force coefficient

c_s - Speed of sound [m/s]

C_t - Tangential force coefficient

D - Aerodynamic drag [N]

d_{RW} - Vertical distance rotor-wing [m]

F - Prandtl's tip loss factor

f_d - Wake downward force on the wing [N]

h_{RW} - Horizontal distance rotor-wing [m]

k - Wake empirical factor

L - Aerodynamic lift [N]

L_2, L_3, L_4 - Four-bar linkage mechanism system theory constants

M - Mach number

N_b - Number of rotor blades

P - Power [W]

P_i - Induced power [W]

P_0 - Profile power [W]

p_N - Normal component of total airfoil force [N]

p_T - Tangential component of total airfoil force [N]

Q - Torque [N·m]

r - Radial axis [m]

R - Rotor radius [m]

S - Wing geometric planform area [m^2]

T - Thrust [N]

T_g - Thrust in pseudo ground effect [N]

T_∞ - Thrust out of pseudo ground effect [N]

U - Total velocity [m/s]

U_a - Axial velocity [m/s]

U_P - Perpendicular inflow velocity [m/s]

U_t - Tangential velocity [m/s]

U_T - Transverse inflow velocity [m/s]

U_∞ - Flight velocity [m/s]

V_h - Horizontal flight velocity [m/s]

v_i - Induced velocity [m/s]

V_v - Vertical flight velocity [m/s]

w - Main rotor wake velocity [m/s]

W - Weight [N]

x - Position in chord axis [m]

y - Position in wing tip-to-tip axis [m]

z - Position in airfoil thickness axis [m]

Z - Altitude [m]

List of Acronyms

AoA - Angle of Attack

IGE - In Ground Effect

IPGE - In Pseudo Ground Effect

LE - Leading Edge

NACA - National Advisory Committee for Aeronautics

OGE - Out of Ground Effect

OPGE - Out of Pseudo Ground Effect

TE - Trailing Edge

TPP - Tip Path Plane

1 Introduction

1.1 Motivation and goals

Design processes of complex systems are usually long and complicated and they are often composed of various steps. One of the first phases that designers usually go through is the preliminary design. As a result of this preliminary design, designers get some basic information about the performance, geometry or viability of their projects and their correlations, and it is a good basis to get into detail afterwards and reach the final design.

Aerospace vehicles and, specifically, helicopters are an example of these complex machines where a good preliminary design is key for their successful development. However, it is difficult to find open-access tools for people interested in rotary-wing aircraft's design.

The goal of this thesis is to further develop a tool (originally created by another student [1]) whose aim is to work as an open-access and easy Matlab tool for the user to perform some calculations that can provide information about the initial design of rotary-wing aircrafts. With its intuitive interfaces, it can be useful for aerospace designers who want some initial information about their vehicles to make some decisions in future steps, students or people who are just interested in the topic.

Therefore, the objective of this thesis is to improve this tool by adding new functionalities, which are related to the study of compound helicopters' performance. In addition to these new functionalities for the helicopters studies, the creation of a new interface for cyclocopters' performance calculations (based on the codes developed by a previous student [2]) is also under the scope of this thesis.

1.2 Topic overview

1.2.1 Compound helicopters

Helicopters are aircrafts that use rotary-wing systems to produce all the forces required for a stable and controlled flight, i.e. their rotors generate lift, thrust and control forces. Conventional helicopters only use rotors to generate these forces and they are suitable for many kinds of flight operations. However, auxiliary systems can be added to the conventional configuration to improve helicopters performance in specific operations or flight regimes.

The helicopter is the most efficient flying machine in hover and at low speed, but it has some inherent constraints, such as rotor drag, stall and compressibility effects, which limit its speed and efficiency for flights with high advance ratios. However, in the 1950s and 1960, some researches about compound helicopters configurations showed they improve the performance for such advance ratios. [3]

Compound helicopters use auxiliary structural elements, such as wings, or propulsion devices, such as propellers, to improve the aircraft performance. One of the main improvements that compound helicopters configurations can usually achieve is an increase in helicopter maximum flight speeds. There are three main kinds of compound helicopters configurations, depending on the auxiliary elements they use. [4]

The first kind of configuration is the lift compound helicopter, which has a fixed wing added to the airframe. This wing creates lift, so that it carries a fraction of the aircraft weight, therefore offloading the main rotor (it has to generate now a lower vertical thrust to overcome the weight). Moreover, the addition of the wing often decreases the power required by the main rotor for a certain flight operation, due to this offloading and the usual high aerodynamic efficiency of such wings. This allows the helicopter to fly more efficiently under certain conditions of speed and weight or improve its performance for a given power consumption (for instance, increasing the flight speed). [4]

On the other hand, the addition of a wing in lift compound helicopters also has some drawbacks. One of them is the weight penalty it comes with. The wing adds an extra structural weight to the helicopter total weight which has to be overcome by the rotor and the wing. This may lead to an increase in power consumption or a decrease in the useful payload the helicopter can carry. Another relevant disadvantage is that the wing just generates the desired lift force in forward flight (and specially for high flight velocities). In hover and low speed forward flight (like during take off and landing), there is usually an interference between the rotor wake and the flow over the wing which is important to be taken into account. The main rotor wake interacts with the flow over the wing and hits its upper surface, producing a download or a vertical down force on the wing which has to be compensated by the main rotor. This will therefore increase the main rotor thrust and power requirements. Lastly, the wing creates some extra drag which must be compensated by the main rotor, so it has to be tilted more forward. This causes the helicopter pitch to be more nose down, which reduces the wing angle of attack and its lifting capabilities. [4]

An example of a lift compound helicopter is Sikorsky S-67 Blackhawk, a combat prototype helicopter developed in 1970. A picture of this aircraft is shown in Figure 1.1.

The second compound helicopter configuration is the propulsive compound helicopter. In this configuration, one or more propulsive devices, like propellers, are added to the conventional helicopter model. There are two main parts where the propellers may be placed along the helicopter airframe: at the tail, where a single propeller is usually placed, or at the wings (if existing), where two propellers are usually placed (one at each side). The propellers create thrust, so that they carry a fraction of the aircraft total drag, therefore offloading the main rotor (it has to generate now a lower horizontal thrust to overcome the drag). This main rotor offload also reduces the rotor power requirements, which leads to a reduction of the shaft torque and rotation speed needs.

Figure 1.1: Sikorsky S-67 Blackhawk [royalty free image]

This allows the helicopter to reach higher velocities, since the onset of retreating blade stall and compressibility effects in the main rotor is now delayed to higher velocities. [5]

On the other hand, the addition of propellers also has some drawbacks. First, the propellers add some extra weight to the total weight of the aircraft, which increases the vertical thrust requirement (and therefore power requirements) of the main rotor. The vehicle overall power requirements also increase due to the propeller. Moreover, as in the case of lift compound helicopters, an interference between the main rotor wake and the propellers is usually seen, producing undesired download forces and increasing the loads on the blades. This phenomenon specially affects the propellers which are on the wing at low flight speeds and affects the propellers at the tail at high flight speeds. [4]

An example of a propulsive compound helicopter is Sikorsky X2, a prototype of hybrid high-speed helicopter which performed its first flight in 2008. A picture of this aircraft is shown in Figure 1.2.

Both previous configurations are usually combined to make compound helicopters which have both wings and propellers and combine characteristics of both configurations. In this combined compound configuration, the propeller offloads the main rotor of the extra forward thrust it has to generate due to the wing drag, allowing the control of the helicopter pitch to maximize the wing lifting capabilities (the helicopter pitch is less nose down, which increases the wing angle of attack). [4]

An example of a compound helicopter with a wing and a propeller at the tail is Lockheed AH-56 Cheyenne, an American military helicopter developed in 1966 whose production was finally cancelled six years later. A picture of this aircraft is shown in Figure 1.3.

Figure 1.2: Sikorsky X2 [royalty free image]

Figure 1.3: Lockheed AH-56 Cheyenne [royalty free image]

An example of a compound helicopter with wings and two propellers placed on them is the Eurocopter X3, a prototype of hybrid high-speed helicopter which performed its first flight in 2010. A picture of this aircraft is shown in Figure 1.4.

The major recent advances regarding compound helicopters are specially related to experimental studies or analyses of the capabilities of these configurations, so there are not compound helicopters commercially operating currently.

In conclusion, compound helicopters are useful when flying at high forward velocities, which will be analysed and demonstrated later in this document. This greater efficiency at higher speeds allows the vehicle to reduce fuel mass or extend its range for these velocity ranges. Their main

Figure 1.4: Eurocopter X3 [royalty free image]

disadvantages are related to their higher empty weights when compared to simple configurations, which implies higher costs for carrying a specific payload, and their higher aerodynamic complexity. [4]

1.2.2 Cyclocopters

Drones, when compared to conventional aircrafts, usually have smaller dimensions, so one of their main advantages is their low operational costs and their easy use and accessibility. They also have a wide variety of types; for instance, there are fixed-wing and rotary-wing drones. Cyclocopters are a specific type of rotary-wing drones.

A cyclocopter is a rotary-wing system whose blades move parallel to the rotation axis. The angle of attack of each blade cyclically varies according to the mechanism placed on the rotation axis, so that the blades have positive and negative angles of attack at upper and lower positions of each cycle, respectively. The lift and drag forces generated by each blade along the cycle may be decomposed into a perpendicular and a tangential component to the airfoils. The resultant required force of the cyclocopter and its required power are obtained by varying the angle of attack amplitude and phase angle of each cycle. [2]

An example of a cyclocopter with two rotors (and a small conventional one) is shown in Figure 1.5.

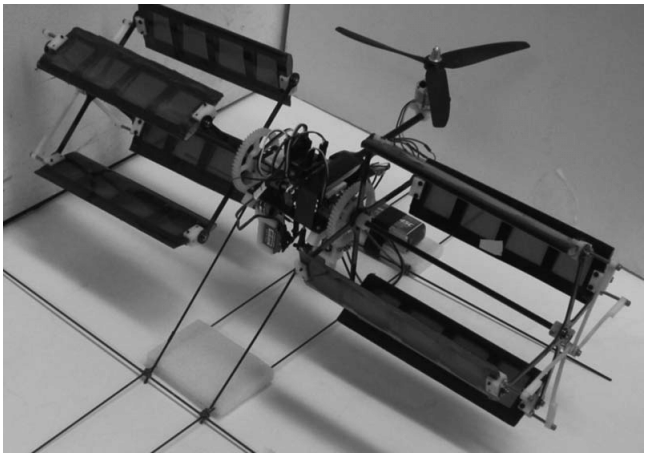

Figure 1.5: Cyclocopter with two rotors [royalty free image]

2 Theoretical background

The understanding of the aerodynamics of wings and propellers has been done using different approaches: analytical theories, numerical methods and experiments. In this work, two different theories have been developed to study the wing's performance and one theory has been developed to study the propeller's performance. Different approaches have been used to study the interactions between the different elements of the compound helicopter. All these theories and approaches are described in detail in this chapter.

2.1 Wing model

In order to study the wing's performance and, specially, its interaction with the main rotor through two different approaches to compare the results afterwards, two different theories were developed: Strip Theory and Thin Airfoil Theory. The user of the tool can choose which theory to use to make the calculations.

2.1.1 Strip Theory

In this theory, which is described in detail in [4], the wing is divided in some strips or slices along the wingspan. In each slice, the aerodynamic forces and moments are calculated to finally integrate the results in all the slices and obtain the resultant wing's forces and moments.

For the development of this theory, several assumptions are considered:

- Each strip does not influence another strip.
- Aerodynamic interactions between the fuselage and wing root are not considered.
- The wing is assumed to be rigid.

Although the Strip Theory does not take into account the 3D effects of the wing, a specific lift distribution along the wingspan and the induced drag have been considered to account for them. Their definition will be presented later in this document.

First, the velocity component in the reference horizontal direction, U_T, and the velocity component in the reference vertical direction, U_P, have to be calculated. Their values will depend on the helicopter speed and the main rotor wake, in case it is interfering with the flow over the wing. Given these velocities, the inflow angle is calculated in the following way:

$$\phi = arctan\left(\frac{U_P}{U_T}\right) \tag{2.1}$$

And the angle of attack is:

$$\alpha = \theta + \theta_{twist} - \phi \tag{2.2}$$

being θ the fixed incidence angle of the wing (pitch angle) and θ_{twist}, the twist corresponding to the slice in study. These angles, together with the airfoil forces and moments, are represented in Figure 2.1 (where there is no twist).

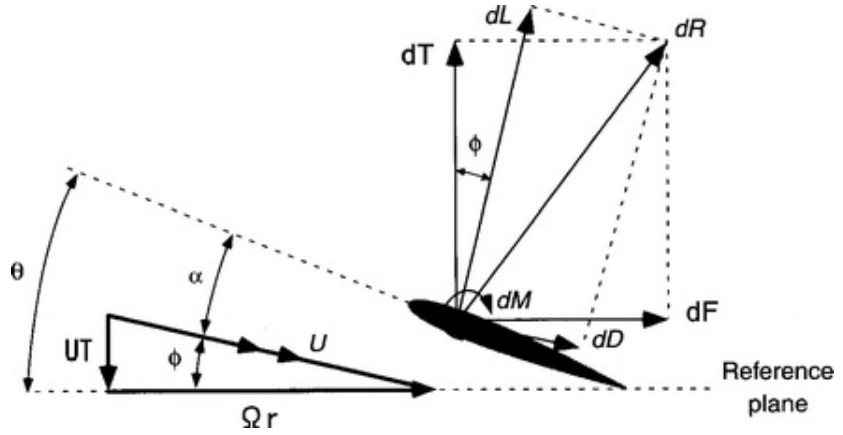

Figure 2.1: Aerodynamic environment at a typical airfoil. [6, pg. 79]

Having the information of the angle of attack, the lift and drag coefficients of each slide are obtained using the information of the lift and drag polar curves ($C_l - \alpha$ and $C_d - \alpha$ curves, obtained from the *xflr5* program [7]) of the corresponding airfoils. And the lift and drag of each slide, which are perpendicular and parallel to the airflow, respectively, have the following expressions in incompressible regime:

$$dL = \frac{1}{2}\,\rho\,U^2\,c\,C_l \tag{2.3}$$

$$dD = \frac{1}{2}\,\rho\,U^2\,c\,C_d \tag{2.4}$$

where ρ is the density, c is the chord and U is the total velocity that the slice sees, which is calculated in the following way:

$$U = \sqrt{U_P^2 + U_T^2} \tag{2.5}$$

In order to account for compressibility effects, the Mach number has to be calculated:

$$M = \frac{U}{c_s} \tag{2.6}$$

being c_s the speed of sound. Now, more accurate equations can be used to calculate lift and drag, considering compressible regime:

$$dL = \frac{1}{2}\,\rho\,U^2\,c\,C_l\,/\sqrt{1 - M^2} \tag{2.7}$$

$$dD = \frac{1}{2}\,\rho\,U^2\,c\,C_d\,/\sqrt{1-M^2} \tag{2.8}$$

The previous expressions are valid when the angle of the attack of the strip in consideration is between the maximum and minimum angles of attack of the airfoil (stall angles of attack). For the cases in which they are higher than the maximum angle of attack (positive stall angle) and lower than the minimum angle of attack (negative stall angle), the lift is considered to be zero. Moreover, in these situations, since the angle of attack is significantly high (or low, in the negative case), the wing drag may be approximated by the drag of a flat plate perpendicular to the flow. Therefore, the drag coefficient corresponding to a flat plate perpendicular to the flow is used for these situations, which has the following value [8]:

$$C_d = 1.28 \tag{2.9}$$

Once the lift and drag are calculated for all the slices, they are all integrated along the wingspan to obtain the resultant lift and drag of the wing.

$$L = \int_0^b dL\,dy \tag{2.10}$$

$$D = \int_0^b dD\,dy \tag{2.11}$$

assuming that the y-axis has been chosen as the one passing through the wing tips and being b the wingspan.

2.1.2 Thin Airfoil Theory

In the cases where the airfoil is thin enough and the angle of attack is not so far from zero, Thin Airfoil Theory can be used to study the airfoil performance. In Table 2.1, the ranges of valid angles of attack to apply the Thin Airfoil Theory for some of the airfoils included in the tool are shown [9].

Table 2.1: Range of valid angles of attack to apply Thin Airfoil Theory for some airfoils

Airfoils (NACA)	**Range of validity of α ($^{\mathbf{o}}$)**
0012	-8 to 12
0024	-4 to 4
2412	-12 to 12
23012	-12 to 12
0030	no valid α

The Thin Airfoil Theory simulates the aerodynamic properties of an airfoil with vortex sheets.

A vortex sheet is a continuous vortex distribution of strength γ along the wing chord. Following this theory, which is described in detail in [10], Equation 2.12 for γ is derived:

$$\frac{1}{2\pi U_\infty}\int_c \frac{\gamma(x)}{x_0 - x}\,dx = \alpha - \frac{dz}{dx} \tag{2.12}$$

where U_∞ is the helicopter flight velocity, x is the coordinate along the chord, $\frac{dz}{dx}$ is the airfoil slope with respect to the chord line (airfoil curvature) and α is the wing nominal angle of attack, just defined by the trajectory angle and the wing pitch (including the twist), so that without taking into account the curvature of the airfoil and the wake influence.

Additionally, following the Kutta condition, the vortex strength is zero at the trailing edge because the flow must flow off the surface tangentially. If the following change of variables to a polar system is now applied:

$$x = \frac{c}{2}\left(1 - cos(\theta)\right) \tag{2.13}$$

the following expression for γ is reached:

$$\frac{1}{2\pi U_\infty}\int_0^\pi \frac{\gamma(x) sin(\theta)}{cos(\theta) - cos(\theta_0)}\,d\theta = \alpha - \frac{dz}{dx} \tag{2.14}$$

To reach a solution for γ, the following distribution in the form of a Fourier series can be assumed as an approximation:

$$\gamma(\theta) = 2U_\infty\left[A_0\frac{1 + cos(\theta)}{sin(\theta)} + A_1 sin(\theta)\right] \tag{2.15}$$

where the constants are given by:

$$A_0 = \alpha - \frac{1}{\pi}\int_0^\pi \frac{dz}{dx}\,d\theta \tag{2.16}$$

$$A_1 = \frac{2}{\pi}\int_0^\pi \frac{dz}{dx} cos(\theta)\,d\theta \tag{2.17}$$

As can be deduced from previous expression, $\gamma = 0$ and therefore there is no lift when the airfoil is symmetric at zero angle of attack.

Depending on the helicopter geometry, rotor and wing characteristics and flight conditions, there are three possible situations for the wing with respect to the rotor wake: wing totally outside the wake, wing totally inside the wake and wing partially inside the wake. These three situations are illustrated in Figure 2.2. For instance, the flight velocity is a determining factor for the wing situation with respect to the rotor wake, since low flight velocities will make the wing be inside the wake and high flight velocities will make it be outside the wake.

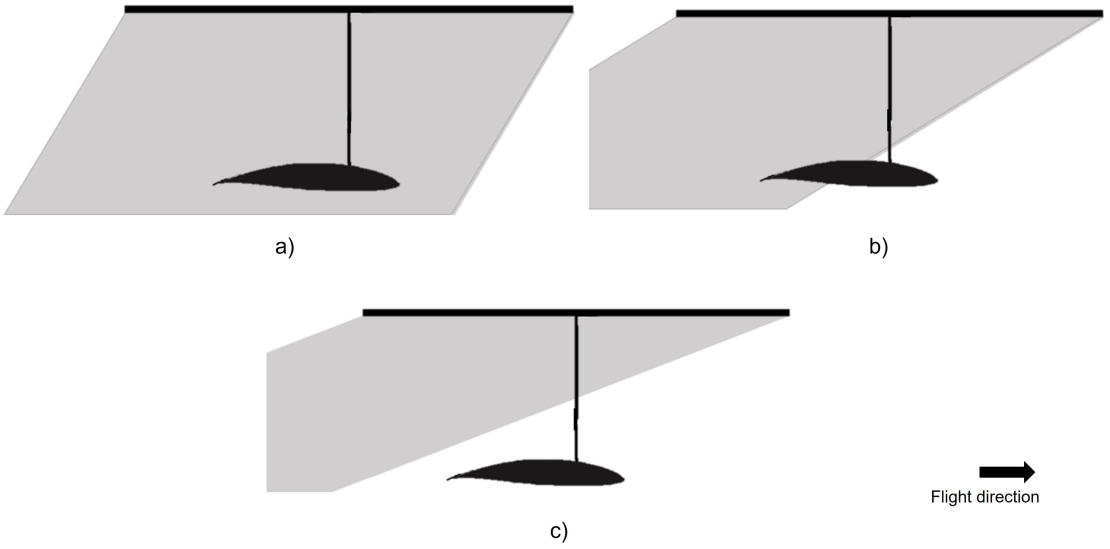

Figure 2.2: Wing situations with respect to the rotor wake (helicopter flying towards the right, with its wake in grey). a) Wing totally inside the wake, b) Wing partially inside the wake, c) Wing totally outside the wake

When the incident velocity changes in a point which is between the airfoil leading and trailing edges, like in case the main rotor wake is partially hitting the wing, the point in x-axis where the wake starts hitting the wing, $x = c_{inside}$, must be calculated and transformed to the polar system, $\theta = \theta_0$, using Equation 2.13:

$$\theta_0 = arccos\left(1 - 2\frac{c_{inside}}{c}\right) \tag{2.18}$$

Consequently, the Thin Airfoil Theory coefficients can be determined in this way for this situation [5]:

$$A_0 = \alpha - \frac{1}{\pi}\int_0^{\pi} \frac{dz}{dx}\, d\theta - \frac{1}{\pi}\int_{\theta_0}^{\pi} \frac{w}{U_\infty}\, d\theta \tag{2.19}$$

$$A_1 = \frac{2}{\pi}\int_0^{\pi} \frac{dz}{dx} cos(\theta)\, d\theta + \frac{2}{\pi}\int_{\theta_0}^{\pi} \frac{w}{U_\infty} cos(\theta)\, d\theta \tag{2.20}$$

being w the vertical component of the main rotor wake velocity that hits the wing. Therefore, the effect of the rotor wake hitting the wing must be added to the effect of the airfoil curvature for the points located inside the wake. As can be deduced, in these cases the lift can be different from zero although the airfoil is symmetric at zero nominal angle of attack, since the wake changes the local flow angles in the points under its influence.

For the case of symmetric airfoil ($dz/dx = 0$), the previous expressions of the coefficients can be directly integrated, obtaining:

$$A_0 = \alpha + \frac{w}{U_\infty}\left(\frac{\theta_0}{\pi} - 1\right) \tag{2.21}$$

$$A_1 = -\frac{2}{\pi}\frac{w}{U_\infty} sin(\theta_0) \tag{2.22}$$

With these coefficients, the total angle of attack (which takes into account the trajectory and pitch angles, the arirfoil curvature and the effect of the rotor wake on the wing), α_t, and the total velocity, U, are calculated using the following expressions:

$$\alpha_t = A_0 + \frac{A_1}{2} \tag{2.23}$$

$$U = \sqrt{U_\infty^2 \left(1 + tan^2(\alpha)\right)} \tag{2.24}$$

With the information of the total angle of attack and the total velocity, the lift and drag of the wing can be calculated. For the lift coefficient, the following expression is used:

$$C_l = 2\,\pi\,\left(\alpha_t - \alpha_{ZL}\right) \tag{2.25}$$

where α_{ZL} is the zero-lift angle of attack of the airfoil (angle of attack for which there is no lift generation), which is obtained from the airfoil data.

The strips' drag coefficients are directly obtained from the drag polar curves of the corresponding airfoils and the final wing performance is studied in the way described in the previous section, defined by Equation 2.7-Equation 2.11.

2.1.3 Tip losses

Due to the fact that the pressure below the wing is higher than the pressure above the wing, vortex are created at the wing tip (flow circulating from the lower to the upper surface of the wing). This is a wing 3D effect and leads to lift losses at the airfoils near to the tips, resulting in a specific lift distribution over the wingspan. The lift distribution has been assumed to be elliptical, which is the most efficient lift distribution shape. [11] The highest lift is generated at the middle of the wing (being the wing referred to the combination of both semi-wings), i.e. at the semi-wings roots (links to the fuselage), with zero lift at both tips. Therefore, the circulation along the wingspan has the following expression, according to [11]:

$$\Gamma(y) = \Gamma_0 \left(1 - \left(\frac{2y}{b}\right)^2\right)^{\frac{1}{2}} \tag{2.26}$$

being Γ_0 the circulation at the middle of the wing. y-axis has its origin at the semi-wing roots (wing center) and is positive to the semi-wing on the right (according to flight direction).

Another consequence of these vortex is the existence of induced drag. To model the induced drag of the wing, an additional term is added to the drag of the strips which are closest to the wing tips. The induced drag accounts for the drag of the wing due to the formation of the tip vortex (due to lift generation). Following [4], its coefficient is given by:

$$C_{Di} = \frac{\bar{C_L}^2}{\pi \, \epsilon \, AR} \tag{2.27}$$

where $\bar{C_L}$ is the mean lift coefficient of the wing, ϵ is the Oswald efficiency factor and AR is the wing's aspect ratio, given by [11]:

$$AR = \frac{b^2}{S} \tag{2.28}$$

with S the wing geometric planform area.

2.2 Propeller model

2.2.1 Blade Element Momentum Theory

To model the propeller and calculate its performance in forward flight, the Blade Element Momentum Theory with the induction factors method is applied. The Blade Element Momentum Theory integrates the Momentum Theory, which describes a mathematical model of an ideal actuator disk, and Blade Element Theory, which analyses the local events taking place at the actual blade by dividing them into a number of strips or slices and assuming that each blade section acts as a 2D airfoil to generate forces. The lateral boundary of these slices consists of streamlines, i.e. there is no flow across them. [12]

This theory methodology, which is described in detail in [12], requires an iterative process where the iteration variables are the axial and radial induction factors, a and a', respectively. These factors are defined in the following way:

$$a = \left(\frac{4sin^2(\phi)}{\sigma C_n} + 1 \right)^{-1} \tag{2.29}$$

$$a' = \left(\frac{4sin(\phi)cos(\phi)}{\sigma C_t} - 1 \right)^{-1} \tag{2.30}$$

where ϕ is the inflow angle, C_t and C_n are the tangential and normal force coefficients, respectively, and σ is the propeller solidity, defined as:

$$\sigma = \frac{cN_b}{2\pi R} \tag{2.31}$$

being c the chord, N_b the number of blades that the propeller has and R the rotor radius.

The first step in this methodology is the calculation of the velocity components the blade

element sees. Since they depend on both induction factors and there is no enough data to calculate them so far, it is necessary to make an assumption for their values. The velocity seen by a blade element has an axial component and a tangential component:

$$U_a = (1 - a)U_\infty \tag{2.32}$$

$$U_t = (1 + a')\omega r \tag{2.33}$$

where U_∞ is the helicopter velocity, ω is the propeller rotation speed and r is the radial component of the blade element.

Having these velocity components, the inflow angle and the angle of attack can be now calculated in the same way as in Strip Theory, previously explained, therefore using Equation 2.1 and Equation 2.2. To calculate the forces and power, the total velocity is required, so the following expression is used:

$$U = \sqrt{U_a^2 + U_t^2} \tag{2.34}$$

The Mach number should be also calculated in order to account for compressibility effects, using Equation 2.6.

These velocity components and angles are graphically represented in Figure 2.3, where $V_0 = U_\infty$ and $V_{rel} = U$ and there is no twist.

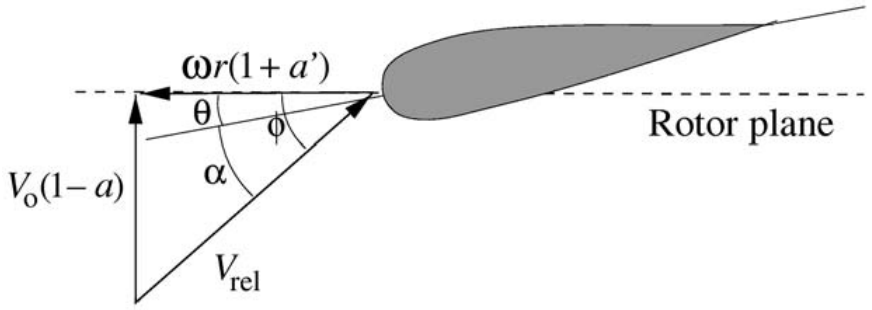

Figure 2.3: Aerodynamic environment at a propeller blade element [12, pg. 47]

Knowing the angle of attack, the lift and drag coefficients for the blade element are taken from the polar curves of the corresponding airfoil. Then, by rotating airfoil lift and drag, the tangential and normal forces (the components of the total blade force which are parallel and perpendicular

to the rotor plane, respectively) are calculated and thus, their coefficients:

$$C_n = C_l\, cos(\phi) + C_d\, sin(\phi) \tag{2.35}$$

$$C_t = C_l\, sin(\phi) - C_d\, cos(\phi) \tag{2.36}$$

as represented in Figure 2.4, where R is the vector sum of the section lift and drag; and p_N and p_T are the normal and tangential components of R, respectively.

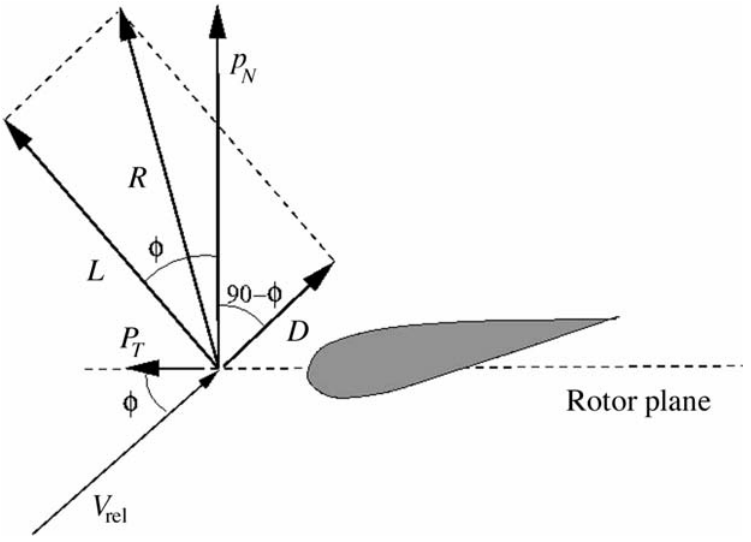

Figure 2.4: Local forces on a propeller blade element [12, pg. 48]

Therefore, the definition of these normal and tangential forces coefficients are:

$$C_n = \frac{p_N}{\frac{1}{2}\,\rho\, U^2\, c} \tag{2.37}$$

$$C_t = \frac{p_T}{\frac{1}{2}\,\rho\, U^2\, c} \tag{2.38}$$

The induction factors can be now computed through their definitions, i.e. using Equation 2.29 and Equation 2.30. If the differences between these results and the values assumed at the beginning of the process are lower than a certain tolerance (defined by the user), the process can continue to compute the total propeller forces and moments. If not, the process must start again with these final values of a and a' as the initial assumption until that situation is achieved.

When the convergence is achieved, with the angle of attack and the velocity, the lift and drag of the blade element are calculated, using Equation 2.7-Equation 2.9. Additionally, the thrust and

torque of the blade element are:

$$dT = dL\,cos(\phi) - dD\,sin(\phi) \tag{2.39}$$

$$dQ = [dL\,sin(\phi) - dD\,cos(\phi)]r \tag{2.40}$$

The total blade element power is composed of different sources of power:

Induced power:

$$dP_i = dL\,sin(\phi)\,r\,\omega \tag{2.41}$$

Profile power:

$$dP_0 = dD\,cos(\phi)\,r\,\omega \tag{2.42}$$

Total power:

$$dP = dP_i + dP_0 \tag{2.43}$$

Once these parameters of all the blades elements are calculated, they are integrated. Finally, an average of these values in all the azimuthal positions which have been considered is made to reach the final values of the propeller thrust and power.

2.2.2 Tip losses

Prandtl proposed a way to correct the assumption of an infinite number of blades. The vortex system of a rotor with a finite number of blades is different from the one that would exist if the number of blades were infinite. There exist lift (and consequently, thrust) losses at the blade sections near to the tip. To address this, Prandtl proposed a correction factor F called Prandtl´s tip loss factor, which is computed with the following expression [12]:

$$F = \frac{2}{\pi}\,arccos\left(e^{-f}\right) \tag{2.44}$$

where:

$$f = \frac{N_b}{2}\frac{R-r}{r\,sin(\phi)} \tag{2.45}$$

being R the propeller radius.

This factor is 0 for the blade section at the tip and tends to 1 while approaching the sections which are near to the propeller axis of rotation. It corrects the section thrust, so the actual (corrected) expression for the thrust of a blade element is:

$$dT = [dL\,cos(\phi) - dD\,sin(\phi)]\,F \tag{2.46}$$

2.3 Ground effect

The ground effect describes the fact that the thrust of a helicopter rotor increases as it approaches the ground for constant power. This effect is relevant in forward flight. As explained in [6], at low forward velocities, a region of flow recirculation is created upstream of the rotor and may throw ground material up that the rotor may ingest. As forward velocity increases, the recirculation region transforms into a vortical flow region between the ground and the rotor leading edge. This increases the inflow through the actuator disk and, consequently, the induced power, so the collective pitch will have to increase to keep the same altitude as the helicopter transitions into forward flight. Flying at an advance ratio higher than a certain value, a ground vortex is created under the leading edge of the rotor. However, if forward velocity continues increasing, this vortex disappears because the rotor wake is skewed back. Therefore, ground effect is normally neglected for advance ratios higher than 0.1. These phenomenons are graphically represented in Figure 2.5.

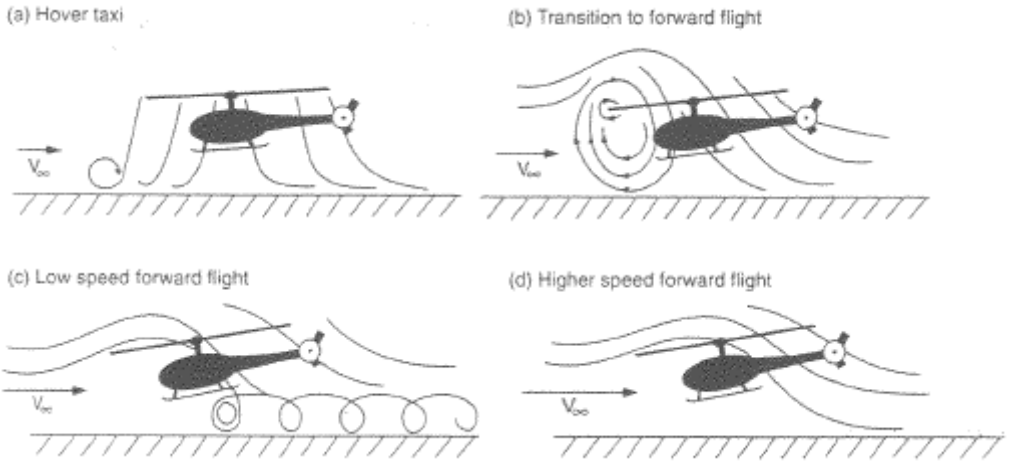

Figure 2.5: Flow in ground effect for a helicopter in forward flight [6, pg. 188]

When flying in hover or at low forward velocities, the ground effect may be beneficial, since a relevant power reduction is experienced. However, the power increases as the helicopter starts flying faster because of the flow recirculation at the leading edge of the rotor disk and its consequent increase of the induced flow at high forward velocities.

In Figure 2.6, the ratio between the actual rotor power (in ground effect and out of ground effect) and the rotor power in hover out of ground effect versus the forward flight velocity is represented. The graph evolution meets the previous explanation, since the power in ground effect (IGE) gets higher than the power out of ground effect (OGE) for velocities higher than 38 kt (70.4 km/h), approximately.

In order to mathematically account for the ground effect in forward flight, the following expres-

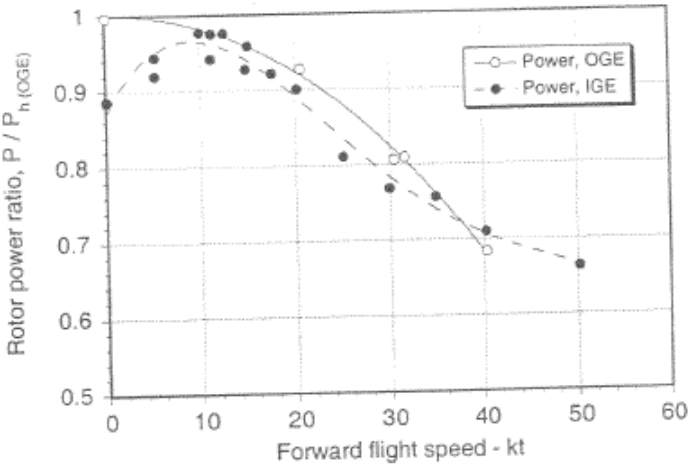

Figure 2.6: Power versus velocity in and out of ground effect for a helicopter in forward flight [6, pg. 189]

sion is used to correct the thrust [13]:

$$T_{IGE} = \frac{T_{OGE}}{1 - \frac{1}{16}\left(\frac{R}{Z}\right)^2 \left[\frac{1}{1+\left(\frac{U_\infty}{v_i}\right)^2}\right]} \tag{2.47}$$

where R is the rotor radius, Z is the helicopter altitude, U_∞ is the forward flight velocity and v_i is the rotor induced velocity.

3 Software implementation

The main computational tool which is under the scope of this work is made up of some other more specific tools which are dedicated to each of the vehicle configurations. Six of these specific tools have been created or completed using the Matlab functionality *appdesigner*. The objective of these tools is to allow the user to make the preliminary design of different types of rotary-wing aircraft by using an easy interface. In general, the user starts defining the flight conditions, top level requirements of the aircraft and some more specific geometrical and aerodynamic parameters that define the different systems and structural elements. For that, the tools have several tabs, dedicated to the different phases of the study or aircraft configurations. Afterwards, the tools make some calculations based on the codes and theories which have been described in the previous chapter of this thesis. Finally, they show the results in a visual way, so that they can be easily analysed and compared.

Three of the tools that take part in this work correspond to basic tools, where the calculations are easier, the study is not so deep (less considerations and theories are taken into account) and more simplification assumptions are made, as will be described in detailed later in this document. These three tools address the following topics: conventional helicopters, coaxial helicopters and tandem helicopters.

Other two tools correspond to detailed tools, where the calculations are more complex, the study is more detailed (a larger number of aspects are considered and taken into account) and less simplification assumptions are made (so the calculations and their results are closer to reality), as will be described in detail later in this document. These two tools address the following topics: conventional helicopters and coaxial helicopters.

The last tool created is the one that studies cyclocopters. In this case, only the tool interface (and its corresponding layout code) was developed, since the codes which the calculations are based on have been developed as part of a different thesis [2].

Besides these tools completions and creations, the ground effect has been added to all the calculations performed by the detailed tools, not only for the compound helicopter calculations, but also for the simple configurations ones, that were originally developed in another work. The factor presented in Equation 2.47 has been applied to the thrust calculated by the codes to get the actual thrust in ground effect.

First, this chapter describes the way in which the main rotor wake interference with the compound helicopters elements (wing and propeller) has been addressed in this work, including the approximations and assumptions this study is based on. Later, the different tools that have been developed will be described in detail, dividing this explanation in three subsections: basic tools, detailed tools and cyclocopter tool.

3.1 Main rotor wake interferences

3.1.1 Interaction of the wake with the wing

The expressions for the velocities in the horizontal and vertical reference direction (in pure forward flight) are different depending on whether the main rotor wake, w, is interfering with the wing or not. In case they are not in contact, these expressions are:

$$U_p = 0 \tag{3.1}$$

$$U_t = U_\infty \tag{3.2}$$

and in case the wake is in contact with the wing:

$$U_p = w \cdot sin\left(\chi + \alpha_{TPP}\right) \tag{3.3}$$

$$U_t = U_\infty + w \cdot cos\left(\chi + \alpha_{TPP}\right) \tag{3.4}$$

being U_∞ the helicopter flight velocity, χ the wake angle and α_{TPP} the main rotor tip path plane angle with respect to the incident velocity direction. α_{TPP} and its sign criteria are represented in Figure 3.1.

The way of calculating the main rotor wake velocity, w, to model the aerodynamic download on the wing due to its proximity to the rotor is the following:

$$w = k\, v_i \tag{3.5}$$

where v_i is the mean induced velocity of the main rotor disc and k is an empirical factor. This factor is one of the tools' inputs, so it is chosen by the user. However, a value of $k = 1.5$ is set as the default one to match the 10% download in hover that was measured in an experimental testing of the V-22. [4] Just the vertical component of w is considered to study the rotor-wing interaction, since the wing receives the rotor wake just from the vertical direction (because the rotor is just above it).

The wake angle, χ, is defined as the angle between the edge of the main rotor wake and the direction which is perpendicular to the rotor. This angle, together with some other geometrical parameters, is illustrated in Figure 3.2.

In Figure 3.2, R is the main rotor radius, d_{RW} is the vertical distance between the main rotor rotation axis and the wing chord, c_{wing} is the wing chord and c_{inside} is the coordinate along the chord axis of the point where the wake starts hitting the wing. In addition, χ_1 and χ_2 are just

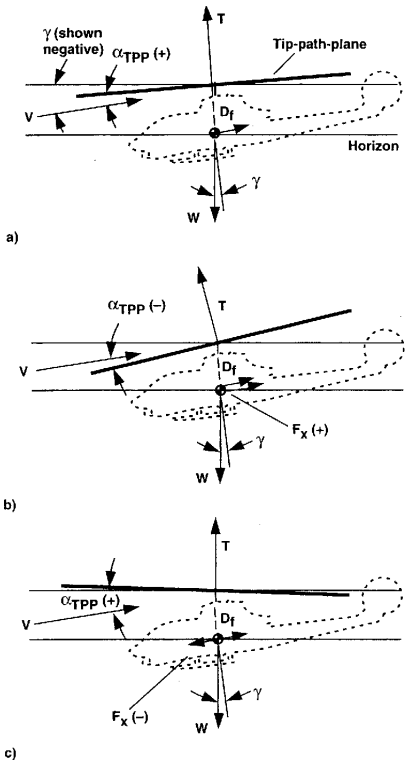

Figure 3.1: Main rotor tip path plane angle and its sign criteria. In a) and c), $\alpha_{TPP} > 0$ because the incident flow hits the bottom part of the rotor and in b), $\alpha_{TPP} < 0$ because it hits the top part of the rotor. [14, pg. 14]

reference angles: the ones between the lines linking the rotor tip with the wing leading edge (LE) and trailing edge (TE), respectively, and the direction which is perpendicular to the rotor.

Both χ and α_{TPP} are calculated in the main rotor code.

Looking at Figure 3.2, c_{inside} can be calculated, using geometrical considerations, with the following expression [5]:

$$c_{inside} = tan(\chi + \alpha_{TPP})\, d_{RW} - R + \frac{c_{wing}}{4} - h_{RW} \tag{3.6}$$

where h_{RW} is the horizontal distance between the main rotor rotation axis and the wing aerodynamic centre (which is considered to be zero in Figure 3.2).

Applying the previous equation and therefore obtaining c_{inside}, θ_0 may now be calculated using Equation 2.18, and the rest of the expressions of the Thin Airfoil Theory presented in Section 2.1.2 can be used to study the wing performance.

As described in previous paragraphs, the interaction between the main rotor wake and the wing can be directly studied using Thin Airfoil Theory, for any percentage of the wing inside the wake. However, the situation in which the wake just hits a part of the wing (the wake edge is at some point between the leading and trailing edge of the wing, as illustrated in Figure 3.2) can not be

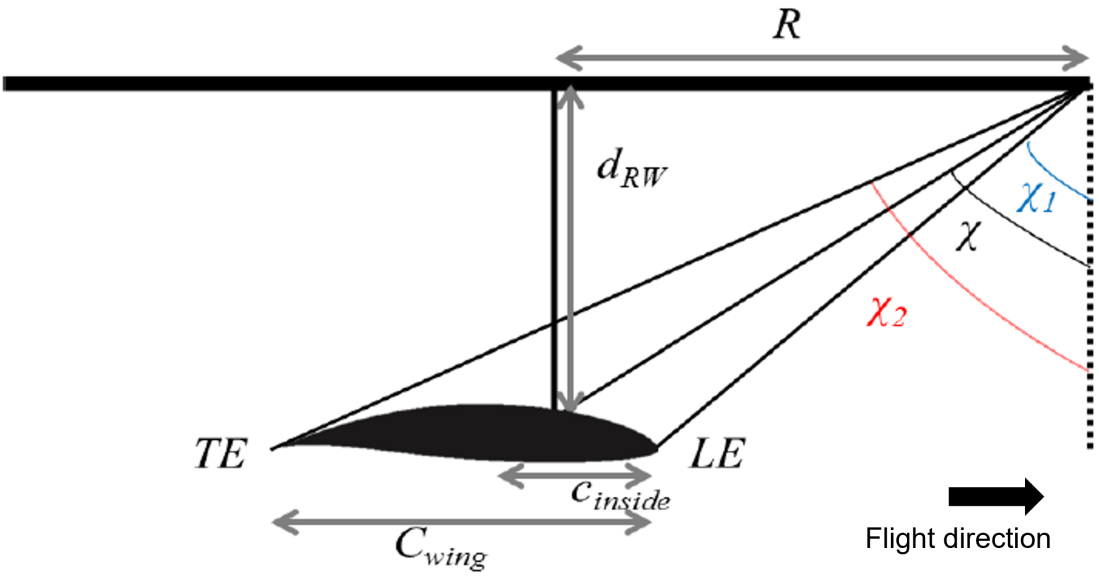

Figure 3.2: Geometrical parameters involved in the interaction between the main rotor wake and the wing (helicopter flying towards the right). [5, pg. 36]

easily modelled using Strip Theory. Therefore, a decision was made in order to get an approach to study this case using Strip Theory in this work.

This approach consists mainly in an interpolation of the results of the lift and drag generated by each wing strip. First, the lift and drag generated by the strip as if the edge of the rotor wake passed through the wing leading edge (so that the whole wing is inside this wake) are calculated. Then, the lift and drag generated by the strip as if the edge of the rotor wake passed through the wing trailing edge (so that the whole wing is outside this wake) are calculated. Finally, the required result is figured out by interpolating the two previous results basing on the percentage of the wing located inside the wake, taking into account that the first result corresponds to 100% and the second one corresponds to 0%.

Since the wake interaction makes the lift of the wing strips be lower (due to the increase that the inflow angle experiments and its consequent decrease of the angle of attack), the first lift result (100% of the wing inside the wake) is generally lower than the second one (0% of the wing inside the wake), so the lift decreases as the percentage of the wing located under the influence of the wake increases, as achieved with this interpolation method and justifying the use of this approach.

Another effect of this interaction between these two elements is that the wing experiences a downward force because of the main rotor wake hitting its upper surface. This effect is already considered by Thin Airfoil Theory, so nothing must be added to contemplate this effect. However, this effect is not taken into account when using the Strip Theory methodology which has been explained in the previous section. To solve this issue, a downward vertical force is added to the forces involved in the strip performance. This force, f_d, uses the drag coefficient corresponding to

a flat plate perpendicular to the flow [8], indicated in Equation 2.9, and the vertical component of the wake velocity:

$$f_d = \frac{1}{2}\rho\ (c - c_{inside})\left[w \cdot sin\left(\chi + \alpha_{TPP}\right)\right]^2 \cdot 1.28 \tag{3.7}$$

Once these parameters of all the wing strips are calculated, they are integrated to get the total downward force. The component of this force in the lift direction is subtracted to the lift result. The component of this force in the drag direction is subtracted to the drag result.

Another consequence of the proximity of the rotor and the wing to be taken into account is the pseudo ground effect experimented by the rotor because of the wing existence. [13] The wing acts as a surface just below the rotor, so similar consequences to the ground effect's ones are experienced and a thrust increase is consequently seen, especially when the wing area is significant compared to the area of the rotor. To model this effect, the expression showed in the previous chapter is used, Equation 2.47, using the distance between the rotor and the wing instead of the aircraft altitude.

$$T_{IPGE} = \frac{T_{OPGE}}{1 - \frac{1}{16}\left(\frac{R}{d_{RW}}\right)^2 \left[\frac{1}{1+\left(\frac{U_\infty}{v_i}\right)^2}\right]} \tag{3.8}$$

where IPGE means *In Pseudo Ground Effect*, OPGE means *Out of Pseudo Ground Effect* and d_{RW} is the vertical distance between the rotor and the wing. As explained in [13], this expression is just theoretical and it properly represents the reality for values of the distance rotor-wing which are not too small. For too low values of this distance, the factor T_{IPGE}/T_{OPGE} becomes too high and does not correspond to the real performance. Because of that, this factor has been limited to take a maximum value of 2: when the distance rotor-wing is so low that the factor is higher than 2, the code uses a value of 2 for the calculations. This is a common assumption because of the theoretical nature of Equation 3.8, which makes it not suitable to model this effect in an accurate way when the value of the factor is too high (higher than 2).

Since the wing area is commonly lower than the rotor area and it sometimes locates at a certain distance from the rotor axis along the fuselage direction, the whole rotor is not usually influenced by this effect, but only the part which is just above the wing area. To take into account this aspect, the thrust factor T_{IPGE}/T_{OPGE} which is actually used in the calculations is the result of an interpolation between 1 (which would correspond to 0% of the rotor area above the wing area, i.e. no pseudo ground effect experienced) and the factor resulting from Equation 3.8 (which would correspond to 100% of the rotor area above the wing).

Once the real ground effect thrust factor and this pseudo ground effect factor are both calculated, they are multiplied to get the total factor which is used to calculate the actual thrust (influenced by both effects).

3.1.2 Interaction of the wake with the propeller

Although the distance between the main rotor and the propeller (located at the helicopter tail) is generally higher than that between the rotor and the wing, there also exists an interaction between these two propulsive elements of the compound helicopter.

When the helicopter flies in forward flight regime, the wake of the main rotor is pushed back, so it will reach the propeller located at the tail or, at least, a part of it. This phenomenon becomes especially remarkable when the forward flight velocity is significantly high, since the wake angle would be high as well and then the wake will move almost horizontally towards the helicopter tail, reaching the propeller in a more probable way.

Because of that, in the cases where this interaction is especially relevant, the most important wake velocity component is the horizontal one (which is parallel to the main rotor plane and perpendicular to the propeller at the tail). That is why the vertical component of the velocity has been neglected to define the model and the calculations of this interaction in this work. Therefore, it has been considered that the only part of the rotor wake which the propeller sees and interacts with is its horizontal component, which comes perpendicular to the propeller and hits its full disc or just a part of it.

Consequently, the expression which is actually used for the propeller axial component is the sum of the flight velocity and the horizontal component of the wake velocity, corrected by the axial induction factor. Therefore, instead of Equation 2.33, the equation used in the Blade Element Momentum Theory of the propeller calculations to account for this rotor-propeller interaction is the following one:

$$U_p = (1 + a)[U_\infty + K\, w\, sin(\chi)] \tag{3.9}$$

In some situations, not the whole propeller is inside the rotor wake, but just a certain part of it. Following geometrical considerations which take into account the radius of the rotor and the propeller, the distance between them and the wake angle, the percentage of the propeller area which is actually in contact with the rotor wake is calculated. This percentage, which is the factor K in Equation 3.9, has been multiplied by the wake horizontal velocity when computing the propeller incident velocities. This approximation has been selected to account for the possibility that just a part of the propeller is under the wake influence.

3.2 Basic Tool

Regarding the basic tools, the three of them have the same structure, but there exist some differences related to the specific characteristics of the helicopter configuration they address. Because of that, the first thing that the user should do if he has decided to use a basic tool is choosing which of the tools to take, depending on the helicopter configuration he is interested in. In this

thesis, three new tabs were created inside each of the three basic tools to analyse the different compound helicopter configurations which were described in the introduction: the first tab studies lift compound helicopters, the second one analyses propulsive compound helicopters and the third tab calculates the performance of lift-propulsive compound helicopters (with both wing and propeller).

First, whatever the tool chosen, the user has to pass through the first tabs, which were developed in another thesis [1], but their results are necessary for the analysis made by the tabs developed in this work. In the first two tabs, the user specifies the general dimensions and the top level requirements of the helicopter. In the next three tabs, the user designs the main rotor and the tail rotor and sees the performance results (thrust, power, pitch and different power plots) for the helicopter without any wing or propeller (no compound helicopter). These results are necessary for the calculations of the compound helicopter configurations, since they act as the first iteration for some of the iterative processes that the codes require.

The last three tabs correspond to the ones that study the performance of compound helicopters, which have been developed as part of this thesis.

The aspects that make these tools be called basic and what differentiate them from the detailed tools are the following simplifications and suppositions:

- The wing geometrical characteristics (chord and airfoil) are constant along the wingspan.
- The wing has no twist.
- For the wing aerodynamics calculations, just the Strip Theory can be used, since the Thin Airfoil Theory is not included in the basic tools' codes.
- The wing tip losses are not modelled, so the lift is considered constant along the wingspan.
- The propeller blades geometrical characteristics (chord and airfoil) are constant along the wingspan.
- The propeller blades have no twist.
- The main rotor wake interference with the wing and the propeller is not modelled.
- The ground effect and the pseudo ground effect induced by the wing are not considered.

Due to these suppositions, the results of these basic tools are not expected to completely match the reality, i.e. they will not be so *real* as the detailed tools ones, but they will be a good first approximation useful to get the order of magnitude of the desired results or to be compared with the detailed tools ones. In the detailed tools, these limitations do not exist, as will be described in detail later in this document.

Conventional helicopter

The first of the tabs created is used to perform the calculations about the lift compound helicopters, i.e. the helicopters which include a wing, and its layout can be seen in Figure 3.3. There are different panels in this tab and they are composed of several fields. Some of them are editable fields, where the user can write to introduce the inputs of the problem, and others are not editable because they are just used to show the results.

In the first panel, flight conditions, the user introduces the velocity, angle and altitude of the flight which he wants to make the calculations for. Next, in the wing characteristics panel, the user specifies the geometrical and aerodynamic properties of the wing: wingspan, chord, pitch angle (incidence angle), Oswald efficiency factor (for the calculation of the induced drag) and mass. There is another panel where the airfoil that the wing uses is specified, by choosing among the different possibilities included in the drop down (symmetrical and non-symmetrical airfoils, airfoils with a large variety of thickness values and from different standard rules are included). In this panel, the geometry of the chosen airfoil is also represented in the graph included when pressing the *Update airfoil* button. A red error message appears if the chosen airfoil is not found in the database.

After these wing properties fields, the user fills some fields related to some calculation parameters, which are:

- The number of wing strips which is going to be used in the Strip Theory method.
- The factor that the rotor induced velocity is going to be multiplied by to get the wake velocity.
- The number of rotor radial segments where the rotor calculations will be performed.
- The number of angular positions where the rotor calculations will be performed.
- The convergence criteria.
- The maximum number of iterations (when reached, the calculations stop, showing an error message).
- The linear inflow model used for the rotor calculations, which is selected by choosing the preferred one among the several possibilities included in the drop down.

When all these flight conditions, wing properties and calculation parameters are set, the *Calculate* button is pressed to perform the calculations. When they are finished, the outcome of the calculations are shown in the results panel, where the user can see the wing lift and drag, the rotor mean thrust, power and torque and the rotor blade root pitch angle.

The second tab is dedicated to the propulsive compound helicopters calculations, i.e. the helicopters which include a propeller at its tail, and its layout can be seen in Figure 3.4. The

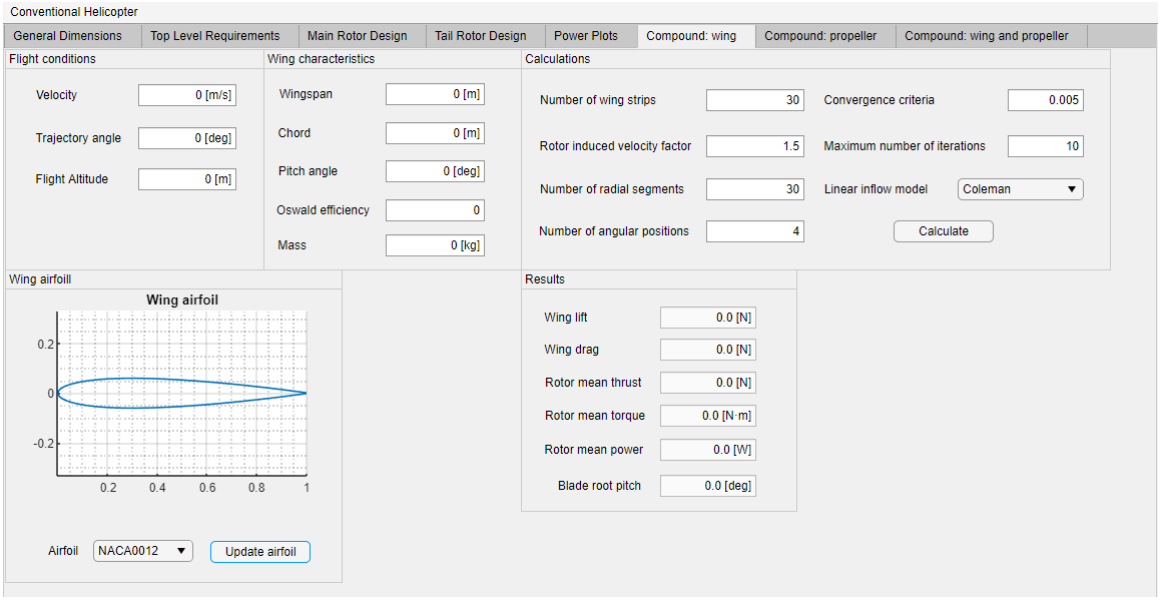

Figure 3.3: Lift compound configuration tab of the conventional helicopter basic tool

different fields this tab includes generally follow the structure of the previous tab, but there are some differences due to the characteristics of this new helicopter configuration.

In the first group of edit fields, the user can specify the geometrical and aerodynamic characteristics of the propeller: number of blades, radius, root cut-out, blade mass distribution, rotational velocity, blade pitch and chord. The flight conditions panel contains the same fields as in the tab previously explained, as well as the tab for selecting the blades airfoil, which also includes a graph to geometrically represent the shape of the selected airfoil. The calculations panel contains the same fields as in the previous tab, but changing the wing calculations parameters by the propeller ones, which are the propeller radial segments and angular positions where the calculations are to be performed.

As in the previous case, after pressing the *Calculate* button, the tool will run the different codes involved to finally show the results in the corresponding panels: the propeller results panel, which shows the propeller thrust and power, and the main rotor results panel, which shows its thrust, torque, power and blade root pitch.

The third and last tab of this tool is dedicated to the analysis of those helicopters that combine both compound configurations, i.e. they have a wing and a propeller. Its layout can be seen in Figure 3.5. In this case, there are less panels and editable fields in the layout. This is because this last tab takes the geometrical and aerodynamic characteristics of the wing and the propeller from the data introduced in the previous two tabs. This means that it is necessary to pass through the lift compound tab and the propulsive compound tab before performing the calculations of this last tab.

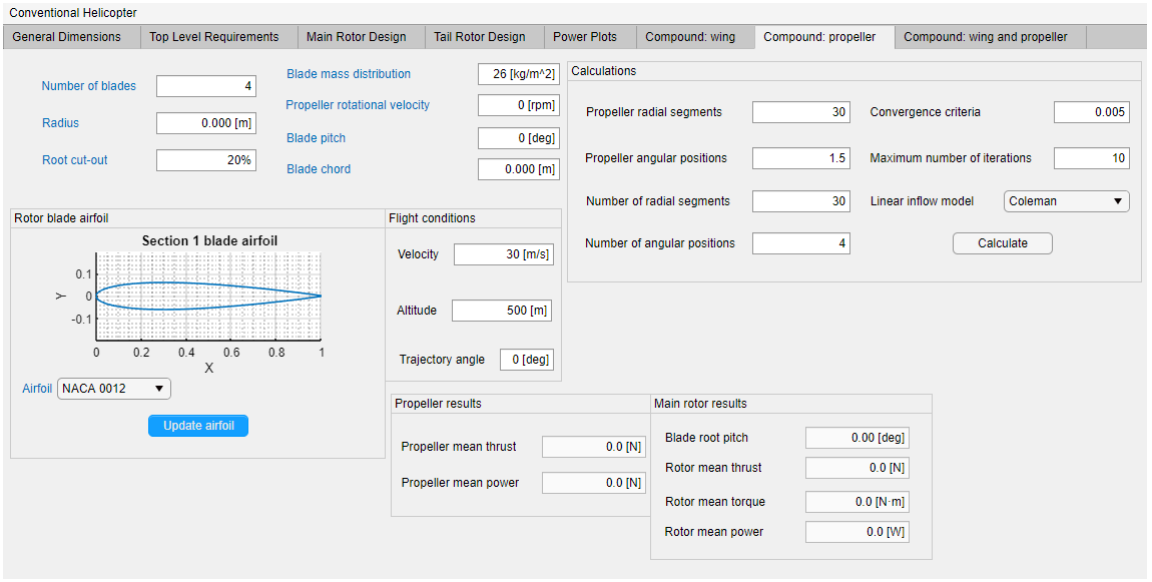

Figure 3.4: Propulsive compound configuration tab of the conventional helicopter basic tool

Therefore, this tab just has the flight conditions panel (including the same three fields as in the two previous tabs) and the calculations panel, which includes both the calculation parameters related to the wing (number of wing strips and rotor induced velocity factor) and to the propeller (number of radial segments and angular positions), so they can be different to the ones introduced in their specific tabs, in addition to the general calculations parameters (convergence criteria and maximum number of iterations).

In the three tabs just described, error messages appear if sonic Mach number is reached for any point on the main or tail rotor or the specified maximum number of iterations is reached. The calculations stop when these situations happen. These messages may be visualized in Figure 3.5.

Coaxial helicopter

The second of the basic tools created is used to perform the calculations of coaxial compound helicopters, i.e. the helicopter with two rotors (one above the other), no tail rotor and the compound device (wing, propeller or both).

The structure of this tool is basically the same as in the conventional helicopter tool: the first tab created is for the lift compound helicopter, the second one is for the propulsive compound helicopter and the third one is for the combined compound configuration. The fields inside each tab are basically the same as in the conventional helicopter tool, with the exception of the fields which show the specific results of the top and bottom rotors. In order to illustrate that, the lift compound tab is shown in Figure 3.6.

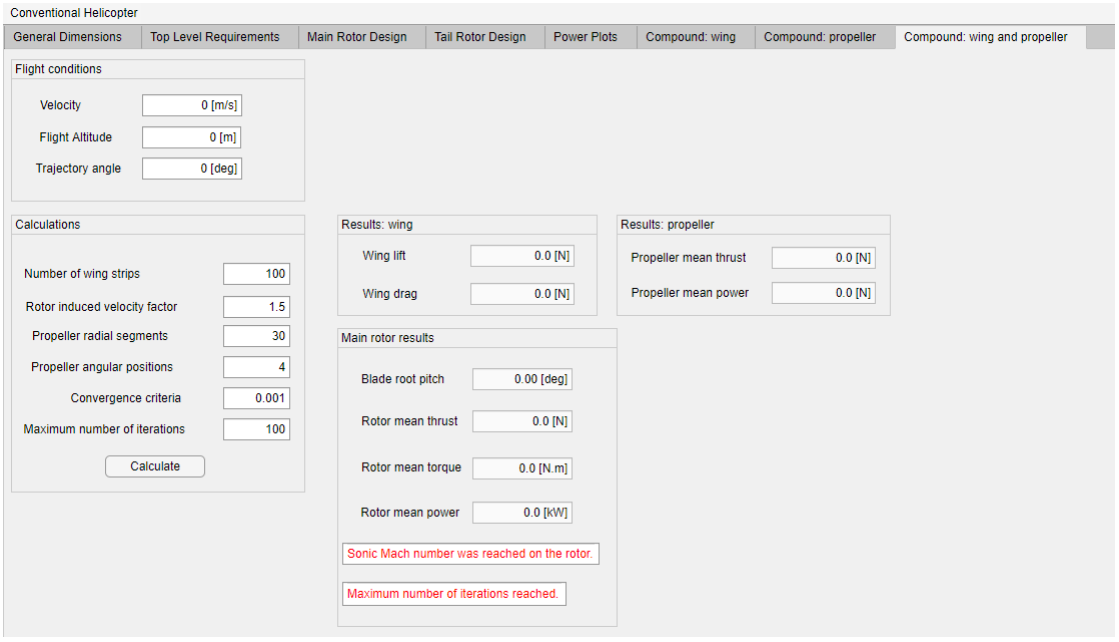

Figure 3.5: Combined compound configuration tab of the conventional helicopter basic tool

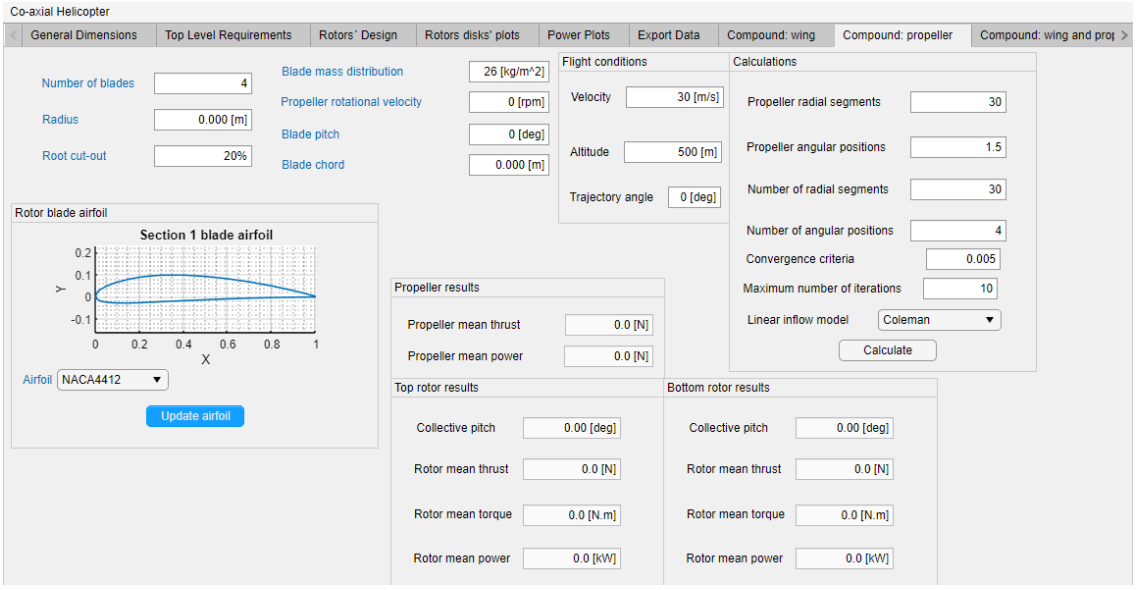

Figure 3.6: Lift compound configuration tab of the coaxial helicopter basic tool

Tandem helicopter

The third of the basic tools created is used to perform the calculations of tandem compound helicopters, i.e. the helicopter with two rotors (one at the front and the other one at the rear part of the vehicle), no tail rotor and the compound device (wing, propeller or both).

The structure of this tool is basically the same as in the conventional and coaxial helicopter tools: the first tab created is for the lift compound helicopter, the second one is for the propulsive compound helicopter and the third one is for the combined compound configuration. The fields inside each tab are basically the same as in the conventional and coaxial helicopter tools, with the exception of the fields which show the specific results of the front and rear rotors. In order to illustrate that, the propulsive compound tab is shown in Figure 3.7.

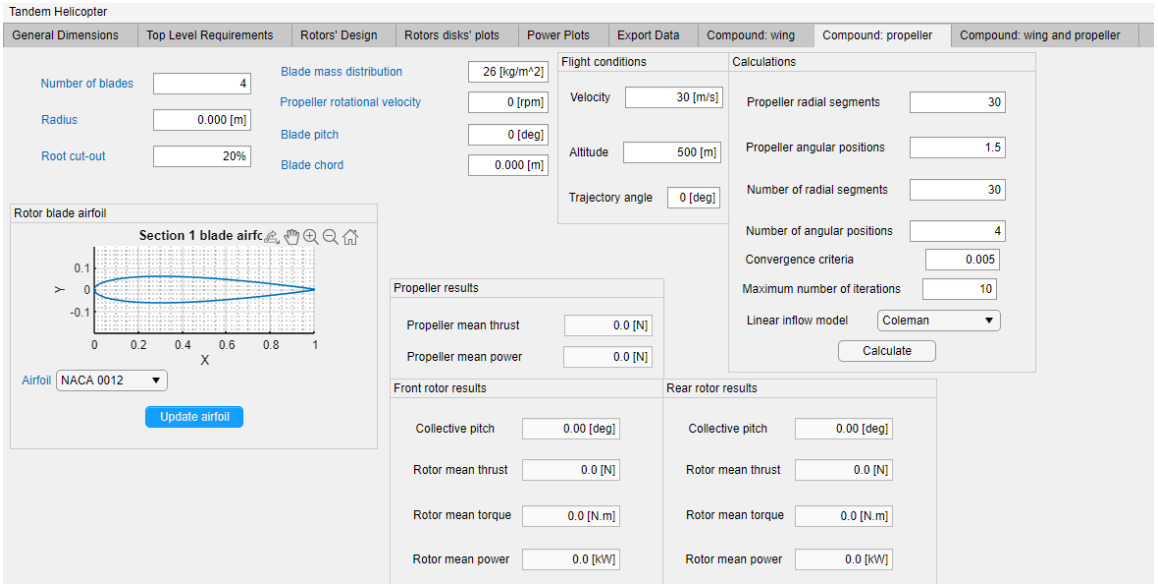

Figure 3.7: Propulsive compound configuration tab of the tandem helicopter basic tool

3.3 Detailed Tool

The detailed tools have the same main structure that the basic tools have, but they are more complex because a higher number of theories are involved in the calculations and less simplifications are made, in order to get more accurate results, closer to reality. In the same way as in the basic tools, the first thing the user must do is choosing the helicopter configuration he wants to study, because there exist two different tools, corresponding to each of the helicopter configurations in study: conventional and coaxial. Three new tabs were also created in each detailed tool: the first one studies lift compound helicopters, the second one analyses propulsive compound helicopters and the third one calculates the performance of the combined compound configuration.

Before reaching the compound configurations tabs, the user must pass through the first tabs of the tools, created in another thesis [1], because their results are necessary for the analysis made by

the tabs developed in this work. These first tabs correspond to the performance calculations of the helicopters without any compound device (the analysis they perform are also more complex and detailed than in the basic tools) and their results act as the first iteration for some of the iterative processes that the compound configurations codes require.

The last three tabs study the performance of compound helicopters, which have been developed as part of this thesis.

The specific aspects that make these tools be called detailed and what differentiate them from the basic tools are the following:

- The wing geometrical characteristics (chord and airfoil) may vary along the wingspan: the user may choose between a constant, linear or parabolic evolution for the chord and airfoil. Furthermore, the wing is divided into two different sections where the chord evolution and airfoil selection may be different.
- The wing may have twist: the user may choose between a constant, linear or parabolic evolution for the twist.
- For the wing aerodynamics calculations, both the Strip Theory and the Thin Airfoil Theory may be used, the user must choose which of them to use.
- The wing tip losses are modelled so the lift is not constant along the wingspan.
- The propeller blades geometrical characteristics (chord and airfoil) may vary along the wingspan: the user may choose between a constant, linear or parabolic evolution for the chord and airfoil.
- The main rotor wake interference with the wing and the propeller is modelled.
- The ground effect and the pseudo ground effect induced by the wing are considered.
- For the lift compound helicopter configuration, the possibility of including just one semi-wing in the vehicle (the wing structure is only at one of the helicopter sides) is included (its benefits will be explained later in the next lines).

As stated in the previous paragraph, the detailed tools allow the user to choose the possibility of including a wing just at one of the sides of the vehicle. The benefits of this approach are caused by the rotor aerodynamics. [15] The usual way of countering the compressibility effects on the advancing rotor blade side (characterized by shock-induced flow separation, high structural vibrations, blade drag and power consumption) is to decrease the rotational speed of the main rotor. The slowed rotor operation comes at the cost of reduced rotor thrust on the retreating blade side due to the existence of reverse flow, which is characterized by flow separation, vortex shedding, and negative sectional blade lift. This reduced lift in the reverse flow region results in reduced overall lift due to the required balance between the advancing and retreating rotor side, that is, zero hub

rolling moment. One of the usual solutions to ensure trimmed forward flight is the combination of two counterrotating rotors in coaxial configuration. However, another possible solution is the addition of a fixed wing on the retreating blade side of the rotorcraft that produces additional lift, countering the rolling moment of the rotor. This configuration reduces the mechanical complexity of the rotor system and the cost of the aircraft. Moreover, control surfaces on the fixed wing add control redundancy to the aircraft, providing performance optimization capabilities and increasing maneuverability. Because of the advantages previously explained, if this strategy is selected for the study, the half wing is considered to be placed at the left side of the fuselage, i.e. retreating blade side (although the side where it is placed does not really affects the code results because it does not address moments issues).

Conventional helicopter

The first of the tabs created is used to perform the calculations about the lift compound helicopters, i.e. the helicopters which include a wing, and its layout can be seen in Figure 3.8. There are different panels in this tab and they are composed of several fields. Some of them are editable fields and others are not editable because they are just used to show the results.

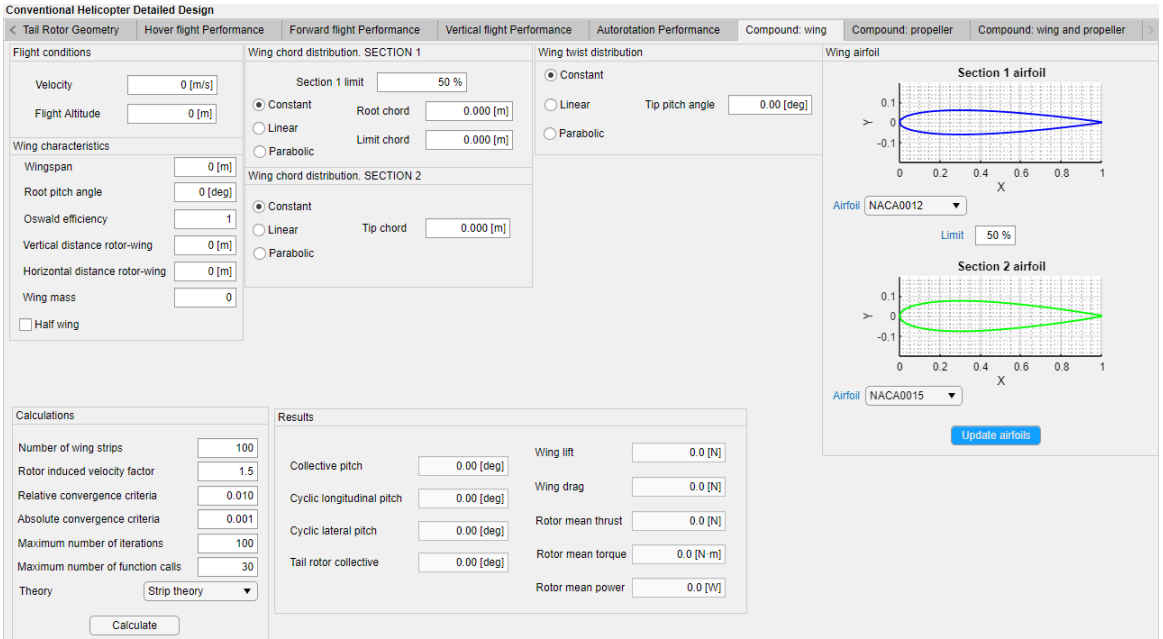

Figure 3.8: Lift compound configuration tab of the conventional helicopter detailed tool

In the first panel, flight conditions, the user introduces the velocity and the altitude of the flight which he wants to make the calculations for. Next, in the wing chord distribution panels, the user specifies the geometrical distribution of the chord along the wingspan (constant, linear or parabolic) and introduces the chord values at both limits of each section in which the wing has been divided. The percentage of the semi-wingspan at which the section change occurs is also

submitted. In a similar way, in the wing twist distribution panel, the pitch distribution must be specified, as well as the pitch at the wing tip (since it is assumed to be zero at the root). There is another panel where the airfoil that each section in which the wing is divided uses is specified, by choosing among the different possibilities included in the drop down. In this panel, the geometry of the chosen airfoil is also represented in the graph included when pressing the *Update airfoil* button. A red error message appears if the chosen airfoil is not found in the database.

In the wing characteristics panel, further wing properties, which are necessary for the detailed calculations, are defined, such as:

- Wingspan
- Root pitch angle: if there is no twist, this angle may be also called as incidence angle.
- Oswald efficiency factor: for the calculation of the induced drag.
- Vertical and horizontal distances between the main rotor hub and the aerodynamic center of the wing: they are necessary for the wake interactions considerations.
- Wing mass: necessary to account for the increase in needed thrust caused by the wing weight addition to the vehicle overall weight.
- Half wing: if this check box is activated, it is considered that the helicopter has just one semi-wing in the left side of the fuselage.

After these wing properties fields, the user fills some fields related to some calculation parameters, which are:

- The number of wing strips which is going to be used in the strip theory method.
- The factor that the rotor induced velocity is going to be multiplied by to get the wake velocity.
- The relative and absolute convergence criteria.
- The maximum number of iterations (when reached, the calculations stop, showing an error message).
- The maximum number of function calls, after which the calculations stop, showing an error message.
- A drop-down to select which of the two theories included in the codes is going to be used to perform the wing calculations: Strip Theory or Thin Airfoil Theory.

When all these flight conditions, wing properties and calculation parameters are set, the *Calculate* button is pressed to perform the calculations. When they are finished, the outcome of the calculations are showed in the results panel, where the user can see the wing lift and drag, the rotor mean thrust, power and torque. Moreover, since the three separated contributions to the blade pitch are

considered in these detailed codes, the collective, cyclic longitudinal and cyclic lateral pitch angles are also shown in this panel, as well as the tail rotor collective (which is the only pitch contribution considered for the tail rotor performance).

The second tab is dedicated to the propulsive compound helicopters calculations and its layout can be seen in Figure 3.9. The different fields this tab includes generally follow the structure of the previous tab, but there are some differences due to the characteristics of this new helicopter configuration.

In the first group of edit fields, the user can specify the geometrical and aerodynamic characteristics of the propeller: number of blades, radius, root cut-out, root pitch, blade mass distribution, rotational velocity and vertical and horizontal distances between the propeller and main rotor hubs (in order to account for the wake interactions considerations).

The flight conditions panel contains the same fields as in the tab previously explained. The panel for selecting the propeller blades' airfoils allows dividing the blades into three different sections and selecting a specific airfoil for each of them; it also includes graphs to geometrically represent the shape of each of the selected airfoils. The calculations panel contains the same fields as in the previous tab, but changing the wing calculations parameters by the propeller ones, which are the propeller radial segments and angular positions where the calculations are to be performed.

As in the previous case, after pressing the *Calculate* button, the tool will run the different codes involved to finally show the results in the corresponding panel: the propeller thrust and power, the main rotor thrust, torque and power, the main rotors collective, cyclic longitudinal and cyclic lateral pitch angles and the tail rotor collective pitch.

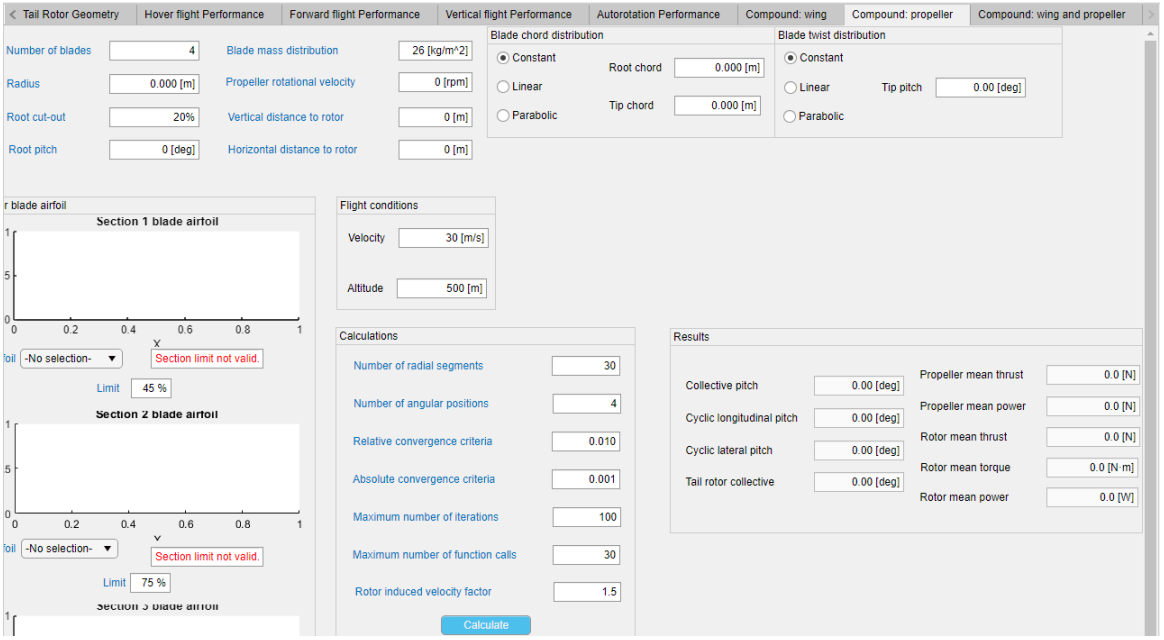

Figure 3.9: Propulsive compound configuration tab of the conventional helicopter detailed tool

The third and last tab of this tool is dedicated to the analysis of those helicopters that combine both compound configurations, i.e. they have a wing and a propeller. Its layout can be seen in Figure 3.10. This last tab takes the geometrical and aerodynamic characteristics of the wing and the propeller from the data introduced in the previous two tabs. This means that it is necessary to pass through the lift compound tab and the propulsive compound tab before performing the calculations of this last tab.

Therefore, this tab just has the flight conditions panel (including the same two fields as in the two previous tabs) and the calculations panel, which includes both the calculation parameters related to the wing (number of wing strips, rotor induced velocity factor and theory to be used) and to the propeller (number of radial segments and angular positions), so they can be different to the ones introduced in their specific tabs, in addition to the general calculations parameters (convergence criteria and maximum number of iterations and function calls).

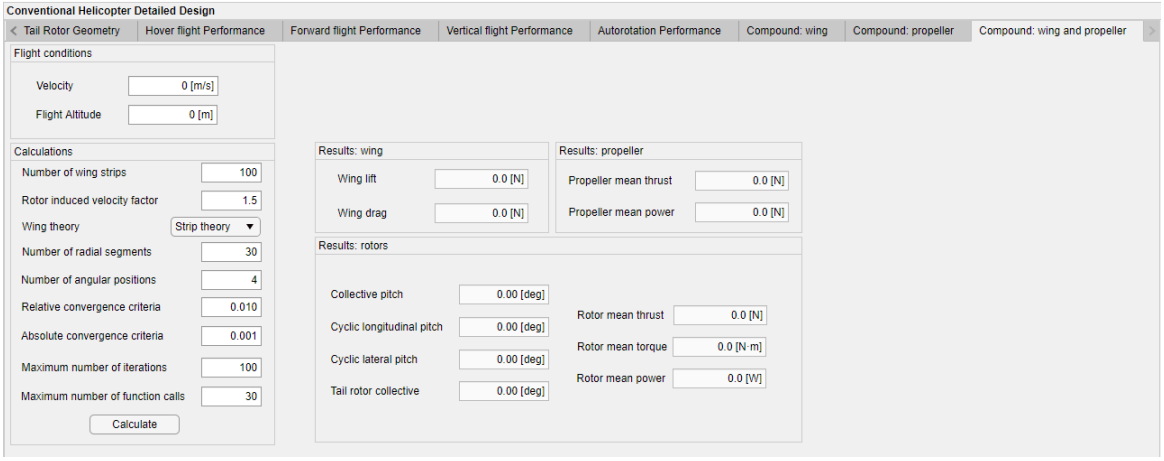

Figure 3.10: Lift and propulsive compound configuration tab of the conventional helicopter detailed tool

In the three tabs just described, error messages appear if sonic Mach number is reached for any point on the main or tail rotor or the specified maximum number of iterations is reached. The calculations stop when these situations happen.

Coaxial helicopter

The second of the detailed tools created is used to perform the calculations of coaxial compound helicopters, i.e. the helicopter with two rotors (one above the other), no tail rotor and the compound device (wing, propeller or both).

The structure of this tool is basically the same as in the conventional helicopter tool: the first tab created is for the lift compound helicopter, the second one is for the propulsive compound helicopter and the third one is for the combined compound configuration. The fields inside each

tab are basically the same as in the conventional helicopter tool, with the exception of the fields which show the specific results of the top and bottom rotors. In order to illustrate that, the lift compound tab is shown in Figure 3.11.

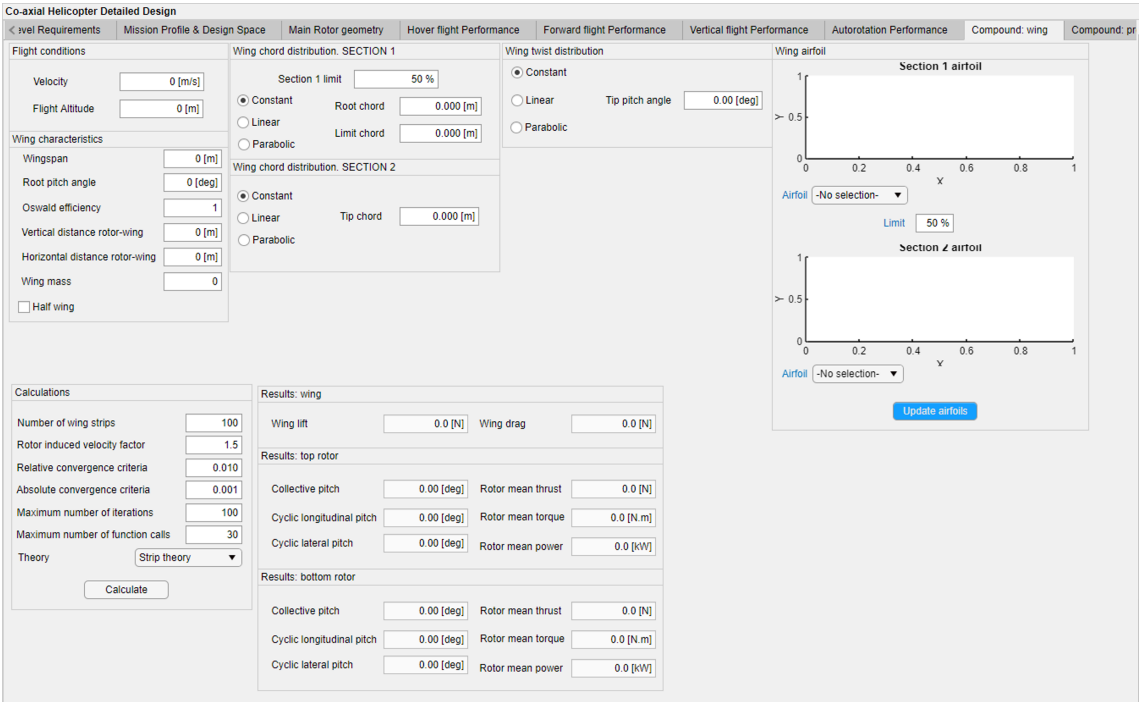

Figure 3.11: Lift compound configuration tab of the coaxial helicopter detailed tool

As previously commented, besides the creation of these new tabs on the detailed tools, the codes corresponding to the calculations in the first tabs of these detailed tools (originally developed as part of another thesis) have also been completed, by adding the ground effect. Therefore, the calculations of the simple (no compound) helicopter performance of the detailed tools take into account the thrust increase that the main rotor experiments due to the vehicle proximity to the ground. This has been modelled by applying the factor presented in Equation 2.47 to the main rotor thrust value that these codes calculate.

3.4 Cyclocopter Tool

The last tool created under the scope of this thesis is dedicated to make the calculations to study the performance of the cyclocopter. Although it is also a rotary-wing vehicle, it is not a type of helicopter as in the previous tools presented, but it is a specific kind of drone. Because of that, this tool is generally different to the previous ones, but it keeps some similarities, mainly related to the flow that the user follows.

As explained in a previous section, just the design and creation of the tool layout (tabs, panels, fields, buttons, etc), together with the code lines which make it work (calls to the programs

containing the equations, assigning the values introduced by the user to the corresponding variables, constraints to some of the numerical fields the user fills, error messages, etc) have been created as part of this thesis. The programs containing the equations and the specific methodologies defined by the theories involved are part of a different thesis [2].

This tool is composed of three different tabs: Single Rotor: hover performance, Single Rotor: forward flight performance and Cyclocopter: pitch calculation.

The first tab which appears when the tool is opened analyses the performance of a single rotor of the cyclocopter in hover. Its layout may be seen in Figure 3.12. First, the user introduces some specific characteristics of the rotor in study, such as: number of blades, radius, blade span, blade chord and rotation speed. In the second panel, the flight conditions are set; as hover is being considered, just the flight altitude is necessary. Once these initial characteristics have been set, the user must choose the theory which the calculations are going to be made with: sinusoidal pitch variation or four-bar linkage mechanism system. There are two different panels, dedicated to each of the theories.

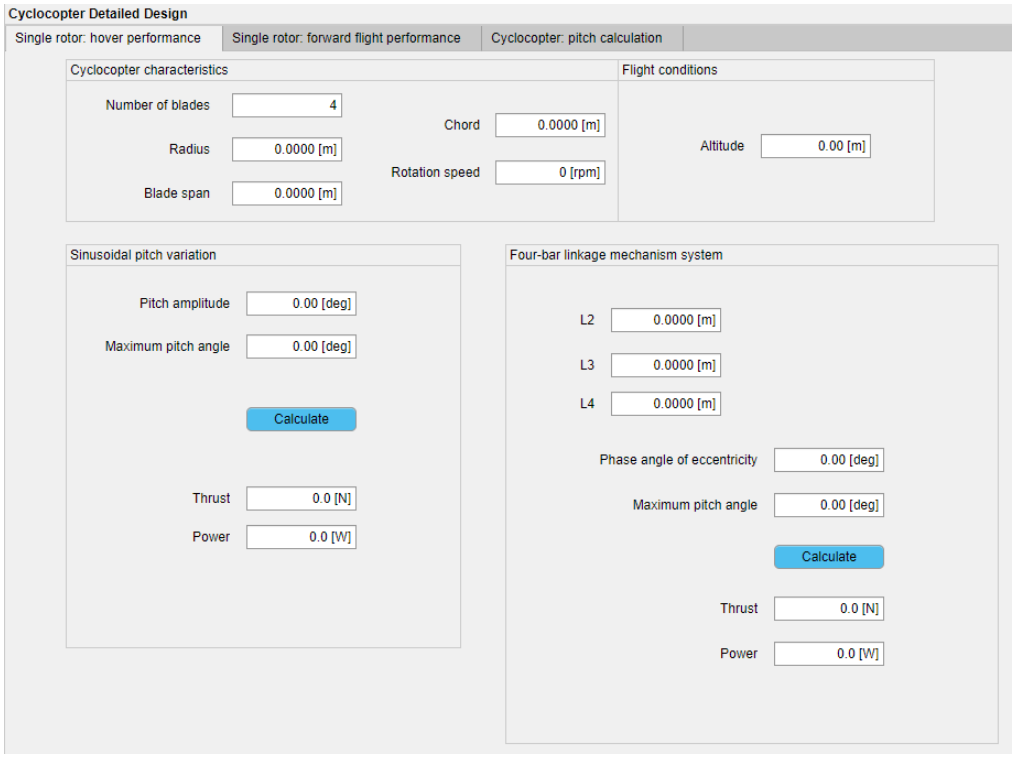

Figure 3.12: Single rotor hover performance tab of the cyclocopter tool

If the theory chosen is sinusoidal pitch variation, the pitch amplitude and the maximum pitch angle must be set as calculation parameters. After that, the *Calculate* button must be pressed to perform the calculations and visualize the result below: the thrust and power of the rotor under the introduced conditions are shown.

Similarly, if the theory chosen is four-bar linkage mechanism system, the constants L_2, L_3 and L_4 (which are characteristic of this theory) must be set as calculation parameters. [2] In the tab code, the following restrictions to this three constants have been set, appearing an error message that stops the calculations if any of them is not satisfied:

$$L_3 > L_4,\ L_3 > L_2,\ L_4 > L_2 \tag{3.10}$$

$$1.01R \geq L_3,\ L_3 \geq R \tag{3.11}$$

$$0.3c \geq L_4,\ 0.3c \geq L_2,\ L_4 > L_2 \tag{3.12}$$

$$0.15c \geq L_2 \tag{3.13}$$

where R is the rotor radius and c is the rotor blade chord.

After that, the *Calculate* button must be pressed to perform the calculations and visualize the result below: the thrust and power of the rotor under the introduced conditions are shown.

The second tab analyses the performance of a single rotor of the cyclocopter in forward flight. Its layout may be seen in Figure 3.13. The only difference of this tab with respect to the previous one is the existence of two fields to introduce the velocity of the cyclocopter in the horizontal and vertical directions (so that a trajectory angle different from zero is allowed), in the flight conditions panel.

Once the calculations for a single rotor have been made, the third and last tab of this tool analyses the whole cyclocopter, integrating the action of all its rotors. The layout of this tab may be seen in Figure 3.14. The first panel (cyclocopter characteristics) is used to select the cyclocopter properties. It includes the same fields as in the previous tabs (the ones corresponding to the single rotor properties) plus the number of rotors, the cyclocopter weight and the cyclocopter flat plate area, which are characteristics of the full cyclocopter.

The cyclocopter weight and flat plate area are necessary for computing the total thrust that the vehicle must develop for performing the selected flight. This calculation has been directly included in the app code and follows the following procedure. First, the cyclocopter structure drag is calculated in the following way:

$$D = \frac{1}{2}\,\rho\,(V_h^2 + V_v^2)\,A_f \tag{3.14}$$

where V_h is the horizontal flight velocity, V_v is the vertical flight velocity and A_f is the introduced

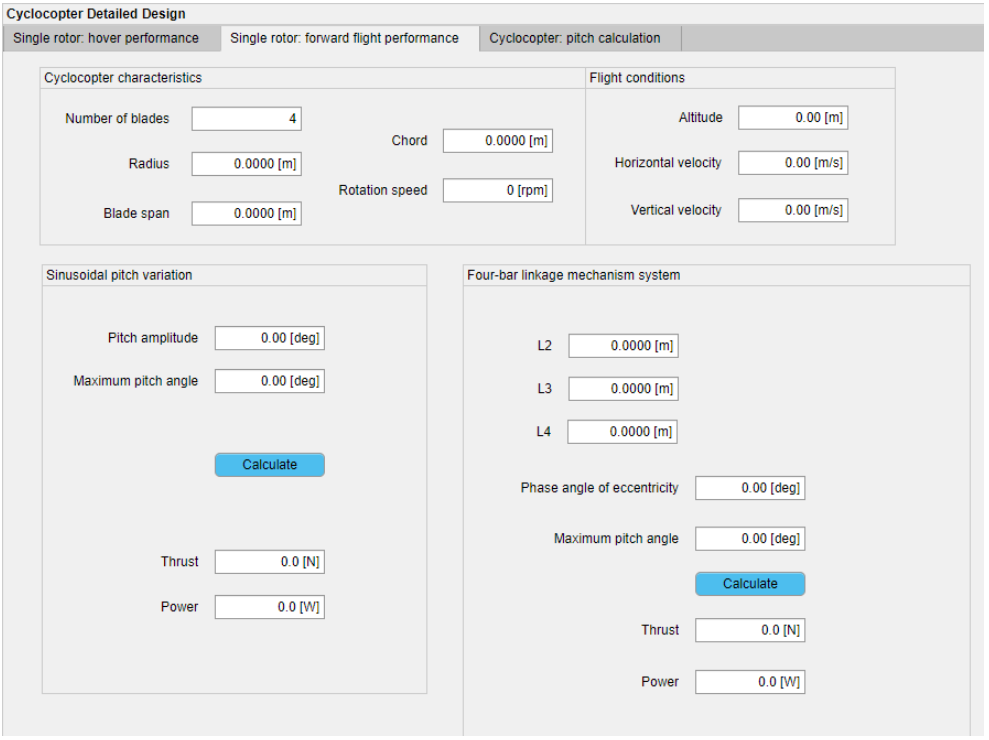

Figure 3.13: Single rotor forward flight performance tab of the cyclocopter tool

flat plate area. With this drag and the cyclocopter weight, the necessary total thrust can be calculated:

$$T_{necessary} = \sqrt{W^2 + D^2} \tag{3.15}$$

where W is the cyclocopter weight. To obtain the necessary thrust that each rotor must develop, this total thrust value is divided by the number of rotors.

Then, the tab is divided in two different parts, related to the hover and forward flight performance. In the hover panel, the user must introduce the flight altitude and some parameters which are necessary for the iterative process that is included in the calculations method: top and bottom limits for the pitch angle amplitude and the thrust convergence tolerance. Basically, the code applies the sinusoidal pitch variation theory, trying all the values for the pitch amplitude included in the defined interval and setting as the final result the one that produces a value for the total thrust whose difference with the necessary thrust for the selected flight conditions is under the specified tolerance. Once the calculations have finished, the rotors pitch amplitude, thrust and power are shown below. The panel dedicated to the calculations of the performance in forward flight follows the same procedure, but including the definition of the vertical and horizontal flight velocities.

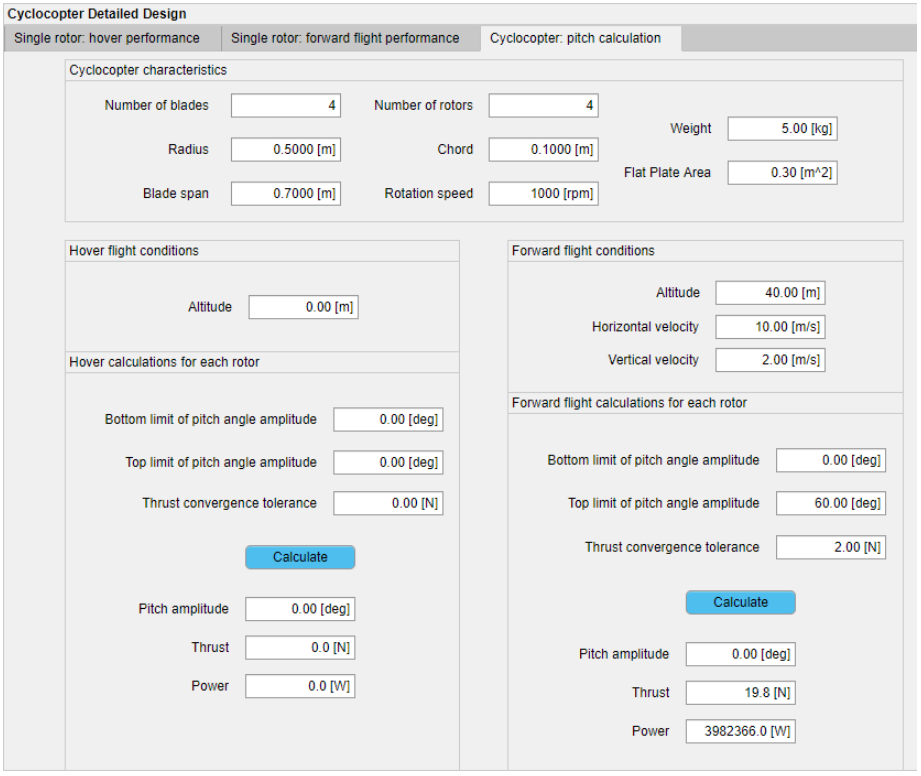

Figure 3.14: Full vehicle performance tab of the cyclocopter tool

4 Validation and Verification

After the theories and procedures used to make the tools and codes of this thesis have been explained, this section is dedicated to test them. In this section, the results generated by the different tools of this thesis are going to be analysed and compared, with other results coming from the tools, results coming from other open-source programs and bibliographic data, with the objective of validating them. This validation and verification is necessary for assuring that the results produced by the work developed are in accordance to the ones generated by others' work and by experiments. In this way, the procedures used and decisions made to develop the work can be considered valid.

This section is divided into four subsections, each of them corresponding to the validation/verification study of one of the parts of this work. The first two subsections are dedicated to the validation of the wing and the propeller alone, without considering their interaction with the rest of the vehicle or the effects they have in the full helicopter. Each of the following two subsections addresses one of the compound configurations studied in this thesis: lift compound and propulsive compound (where an example of a combined compound helicopter is included).

4.1 Wing

For the wing verification, *xflr5* is going to be used, which is a well-known tool composed of various modules for the analysis of airfoils, wings and planes under a great variety of aerodynamic conditions, at low Reynolds numbers. [7] For the analysis, a wing of some determined properties has been selected and introduced in the tool's wing code. Then, the same wing has been modelled in *xflr5* and the results obtained have been compared with the tool ones.

First, the results have been obtained using the wing code of the basic tool. The properties of the selected wing are the following ones: wingspan of 6 m, chord of 0.7 m and NACA0012 as the constant airfoil. The calculations have been performed for several values of the flight trajectory angle and the wing pitch angle (incidence angle) and the results are shown in Table 4.1.

Table 4.1: Comparison of lift and drag results obtained from wing code of basic tool and *xflr5*

Trajectory and pitch angles (º)	Lift (N)			Drag (N)		
	Code	xflr5	Difference (%)	Code	xflr5	Difference (%)
$\theta_{traj} = 0, \theta_{pitch} = 0$	0	0	-	54.7	52.7	3.7
$\theta_{traj} = 0, \theta_{pitch} = 2$	1875.7	1738.6	7.3	69.9	63.2	9.6
$\theta_{traj} = 7, \theta_{pitch} = 0$	6464.7	6058.7	6.3	236.4	200.2	15.3
$\theta_{traj} = 7, \theta_{pitch} = 2$	8585.2	7765.2	9.6	369.6	295.0	20.2

Then, the results have been obtained using the wing code of the detailed tool. For that, a tapered wing (whose chord decreases from root to tip) has been analysed. The properties of the selected wing are the following ones: wingspan of 6 m, chord of 0.8 m at the root and 0.5 m at the

tip, no twist (constant pitch angle equal to 0^{o}) and NACA0012 as constant airfoil. The calculations have been performed for several values of the flight trajectory angle and the results are shown in Table 4.2.

Table 4.2: Comparison of lift and drag results of a tapered wing obtained from wing code of detailed tool and *xflr5*

Trajectory angle (^{o})	Lift (N)			Drag (N)		
	Code	xflr5	Difference (%)	Code	xflr5	Difference (%)
$\theta_{traj} = 2$	1804.2	1682.9	6.7	64.9	58.7	9.6
$\theta_{traj} = 7$	6217.6	5851.0	5.9	219.0	185.9	15.1

In order to further test the possibilities of the detailed tool, a different kind of geometry for the wing has been studied: the twisted wing. The results have been obtained using the wing code of the detailed tool. The properties of the selected wing are the following ones: wingspan of 6 m, chord of 0.7 m, linear twist (pitch angle of 2^{o} at the root and 1^{o} at the tip) and NACA0012 as constant airfoil. The calculations have been performed for several values of the flight trajectory angle and the results are shown in Table 4.3.

Table 4.3: Comparison of lift and drag results of a twisted wing obtained from wing code of detailed tool and *xflr5*

Trajectory angle (^{o})	Lift (N)			Drag (N)		
	Code	xflr5	Difference (%)	Code	xflr5	Difference (%)
$\theta_{traj} = 0$	1480.7	1252.4	15.4	64.2	58.7	8.6
$\theta_{traj} = 5$	6060.0	5679.4	6.3	214.2	179.1	16.4

In summary, it can be seen that both lift and drag of the wing increase with trajectory and pitch angles, due to the subsequent increase of the angle of the attack. The results of the thesis codes are similar to the ones coming from *xflr5*, since the highest error of the studied cases reaches 20%; however, the codes tend to slightly overpredict lift and drag values, with respect to *xflr5*, being the errors higher for the drag. Additionally, the differences between the codes' and *xflr5* results for both lift and drag become higher as they increase. Finally, it can be deduced that the errors are generally lower for the results of the detailed tool than for the basic tool ones, due to the lower number of simplifications considered and the higher number of details included, which makes the study and results closer to the methodology used by *xflr5* (which also performs some assumptions) and to reality.

4.2 Propeller

For the propeller validation and verification, two different sources of data will be used to compare the results obtained with the thesis codes. First, *JBLADE*, a similar software to *xflr5* will be used. *JBLADE* is an open-source propeller design and analysis code which uses the classical

Blade Element Momentum Theory modified to account for the 3D flow equilibrium. [16] For the analysis, several propellers of some determined properties have been selected and introduced in the tool's propeller code. Then, the same propellers have been modelled in *JBLADE* and the results obtained have been compared with the tool ones.

First, the results have been obtained using the propeller code of the basic tool. The properties of the selected propeller are the following ones: 3 blades, radius of 1.6 m, constant pitch of 15^{o}, constant chord of 0.2 m and NACA0012 as the constant airfoil. The calculations have been performed for several values of the flight velocity (perpendicular to the propeller plane of rotation) and two values of the rotation speed. The results of thrust and power are presented in Table 4.4 and Table 4.5, each of the tables showing the results for one of the rotation speed values.

Table 4.4: Comparison of thrust and power results of a propeller with a rotation speed of 1000 rpm and a pitch angle of 15^{o}, obtained from propeller code of basic tool and *JBLADE* for two different flight velocities

1000 rpm	Thrust (N)			Power (W)		
Velocity (m/s)	Code	JBLADE	Difference (%)	Code	JBLADE	Difference (%)
10	2390.1	2027.0	15.2	55122.1	58266.6	-5.7
20	1199.3	1157.2	3.5	38463.4	41208.2	-7.1

Table 4.5: Comparison of thrust and power results of a propeller with a rotation speed of 1500 rpm and a pitch angle of 15^{o}, obtained from propeller code of basic tool and *JBLADE* for three different flight velocities

1500 rpm	Thrust (N)			Power (W)		
Velocity (m/s)	Code	JBLADE	Difference (%)	Code	JBLADE	Difference (%)
10	5824.2	5447.0	6.9	191640.2	216125.7	-11.3
20	4597.9	3851.1	19.4	174160.3	177688.4	-2.0
30	2698.5	2604.4	3.6	129810.5	139077.8	-6.7

Now, the thrust and power results have been obtained for a propeller with a higher value of the constant pitch angle, keeping the rest of parameters constant and also using the basic tool code. The pitch angle selected for this propeller is equal to 30^{o}. The results of thrust and power obtained are shown in Table 4.6.

Table 4.6: Comparison of thrust and power results of a propeller with a rotation speed of 1000 rpm and a pitch angle of 30^{o}, obtained from propeller code of basic tool and *JBLADE* for three different flight velocities

1500 rpm	Thrust (N)			Power (W)		
Velocity (m/s)	Code	JBLADE	Difference (%)	Code	JBLADE	Difference (%)
20	6659.6	5720.0	14.1	273350.1	279200.2	-2.1
30	5212.3	4580.3	12.1	251200.4	255450.5	-1.7
40	3601.7	3495.6	3.0	207870.7	216485.8	-4.0

Looking at the previous tables, it can be seen that the evolutions of thrust and power with

rotation speed and forward velocity are the same for the code and *JBLADE* results, and they correspond to the expected evolutions: both thrust and power increase as rotation speed increases (since the component of the velocity which is parallel to the blade becomes higher) and they decrease as forward velocity increases (due to the perpendicular component of the velocity which is perpendicular to the blade becomes higher, decreasing the angle of attack). Additionally, the errors are of the same order of magnitude for the different pitch angle values in study, so the code behaviour is stable when pitch angle is varied. The thrust and power errors are also of the same order of magnitude. Moreover, a good agreement is found between both sources of results, since the errors are all smaller than 20%, which verifies the tool code results.

The detailed tool code has also been tested by modelling a propeller with a more complex geometry. For this study, a real commercial propeller has been modelled, whose name is *APC Sport Propeller 11x4*. Its geometrical parameters, obtained from [17], have been introduced in the propeller detailed code and are the following ones: two blades, diameter of 27.94 cm, offset of 15%, linear chord distribution (varying from 2.37 cm at the root to 0.28 cm at the tip), linear twist distribution (pitch angle varying from 30^{o} at the root to 9^{o} cm at the tip) and NACA4412 as the constant airfoil. The thrust and power results of the code have been compared with the APC experimental data included in [17] and they are presented in Table 4.7, for different values of the rotation and flight speeds.

Table 4.7: Comparison of thrust and power results of *APC Sport propeller 11x4* obtained from propeller code with experimental data

Rotation	Velocity	Thrust (N)			Power (W)		
(rpm)	(mph)	Code	APC	Error (%)	Code	APC	Error (%)
1000	5	0.049	0.053	8.21	0.14	0.00	-
2000	9.1	0.24	0.28	14.23	1.31	1.49	12.48
3000	15	0.44	0.49	9.95	3.84	5.22	26.50
4000	20.1	0.77	0.87	11.40	9.01	11.93	24.46
5000	25	1.22	1.37	10.66	17.76	23.12	23.17
6000	30	1.76	1.98	10.96	30.69	38.78	20.85
7000	35	2.40	2.71	11.44	48.74	59.66	18.30

Analysing the information presented in Table 4.7, it can be concluded that the power results of the thesis code differ more to the experimental ones than the thrust ones do, since the errors are higher. It may be related to the existence in reality of some other specific sources of power which have not been modeled in the thesis code. Furthermore, the thrust and power errors are generally higher than in the basic tool code comparison with *JBLADE* and it may be caused by two main reasons. The first of them is the fact that the geometrical parameters of the APC propeller had to be slightly adapted to be modeled as tool inputs (so the parameters introduced in the tool are not exactly the same as the real propeller ones). The second reason is the fact that both *JBLADE* and the thesis code consider some simplifications in its study, but in the experimental data, every

factor accounts (and some of them may not have been modeled in the code). The first reason seems to be the most important cause of the errors, since the discrepancies between results are consistent with the increase of the rotation speed. However, all the errors are below 27% and their tendencies meet the experiments.

4.3 Lift compound helicopter

To validate and verify the study of lift compound helicopters, the codes involved in the analysis of helicopters including a wing have been run and tested. For running these calculations, the detailed conventional helicopter tool (lift compound tab) has been selected, since it contains all the theories and considerations regarding lift compound helicopters which have been included in this thesis. Several studies have been made for this validation and verification. First, the study focuses on the verification of one of the key aspects of this thesis: the interaction between the wing and the rotor and how they affect the performance of the other one (some calculations using both theories and some graphs have been made). Then, the Thin Airfoil Theory code has been tested for different airfoils, by comparing the results with the ones obtained with Strip Theory (both results coming from the code developed). Afterwards, the effect of the pseudo ground effect that the rotor experiments due to the existence of the wing just below it is checked. Finally, the whole code structure has been tested by modeling a real helicopter and comparing the results obtained by the tool with experimental data of this helicopter.

In the first verification study, the wing-rotor interaction has been tested. For that, wing lift, wing drag and rotor thrust have been calculated using Thin Airfoil Theory and Strip Theory. The calculations have been performed for four different values of the vertical distance between the rotor axis and the wing aerodynamic center, i.e. four different values of the percentage of the wing which is inside the rotor wake (as the vertical distance between rotor and wing becomes higher, the percentage of the wing which is inside the rotor wake decreases). In this analysis, this percentage is actually the percentage of the chord of the wing root section which is inside the wake. For this study and for the following ones addressing rotor-wing interaction, the horizontal distance between the rotor axis and the wing aerodynamic center has been set to zero.

The wing selected for this study has the following geometrical characteristics: wingspan of 8 m, chord of 1 m, NACA0012 as the airfoil, pitch angle (incidence) of 4^{o} and no twist. The forward velocity of the helicopter in this study is equal to 27 m/s. The results are shown in Table 4.8.

Another way to do the same study is keeping the vertical distance between rotor and wing constant and varying the forward flight velocity of the helicopter, since the percentage of the wing (for this study, wing root section chord) inside the rotor wake decreases as the flight velocity increases (at high velocities, the wake is significantly pushed back, reaching high wake angles and therefore getting further away from the wing). The same study as the one presented in Table 4.8

Table 4.8: Comparison of wing lift and drag and rotor thrust for different values of the percentage of the wing root section chord which is inside the wake by varying vertical distance between rotor and wing, and using both theories

Distance	inside wake		Strip T.	Thin Airfoil T.	Difference (%)
1 m	100%	Wing lift (N)	581.9	568.6	2.3
		Wing drag (N)	33.0	32.9	0.3
		Rotor thrust (N)	60766.3	60759	0.01
1.5 m	73.8%	Wing lift (N)	740.4	660.0	12.2
		Wing drag (N)	32.0	33.8	-5.3
		Rotor thrust (N)	60848.2	60806.3	0.07
1.6 m	20.8%	Wing lift (N)	1043.9	1211.3	-13.8
		Wing drag (N)	30.7	42.4	-27.6
		Rotor thrust (N)	60406.7	60138.3	0.5
2 m	0%	Wing lift (N)	1174.0	1163.0	1.0
		Wing drag (N)	37.2	36.9	0.8
		Rotor thrust (N)	60142.3	60139.1	0.01

has been done, but keeping the vertical distance between rotor and wing fixed to 1.5 m and varying the flight velocity. The wing in study is the same as in the previous analysis. The results are shown in Table 4.9.

Table 4.9: Comparison of wing lift and drag and rotor thrust for different values of the wing root section chord percentage inside the wake by varying flight velocity, and using both theories

Velocity	inside wake		Strip T.	Thin Airfoil T.	Difference (%)
10 m/s	100%	Wing lift (N)	0.0	0.0	0.0
		Wing drag (N)	3557.3	3557.9	-0.02
		Rotor thrust (N)	63176.4	63162.9	0.02
18 m/s	100%	Wing lift (N)	-2012.9	-2054.7	-2.0
		Wing drag (N)	69.4	71.4	-2.8
		Rotor thrust (N)	63378.4	63366.7	0.02
28 m/s	18.1%	Wing lift (N)	1178.3	1487.1	-20.8
		Wing drag (N)	33.5	49.1	-31.8
		Rotor thrust (N)	60216.9	60008.1	0.4
35 m/s	0%	Wing lift (N)	1977.1	1958.6	0.9
		Wing drag (N)	62.8	62.3	0.8
		Rotor thrust (N)	59464.8	59463.9	0.0
50 m/s	0%	Wing lift (N)	4057.6	4019.6	1.0
		Wing drag (N)	129.2	128.1	0.9
		Rotor thrust (N)	57430.6	57543.6	-0.2

In order to deeper analyse how the contact with the main rotor wake affects the wing lift when it is partially inside the wake, the wing detailed code has been run independently of the rest of the tool codes to manually vary the percentage of the wing root section chord which is inside the rotor wake. The vertical distance between both elements and the flight velocity has not been changed, but the wing percentage have been artificially varied. For that, a standard wing similar to the ones of the previous studies have been used. The results of wing lift, using both theories, have been represented, as a function of the percentage inside the wake, in the same graph to be compared and it can be seen in Figure 4.1.

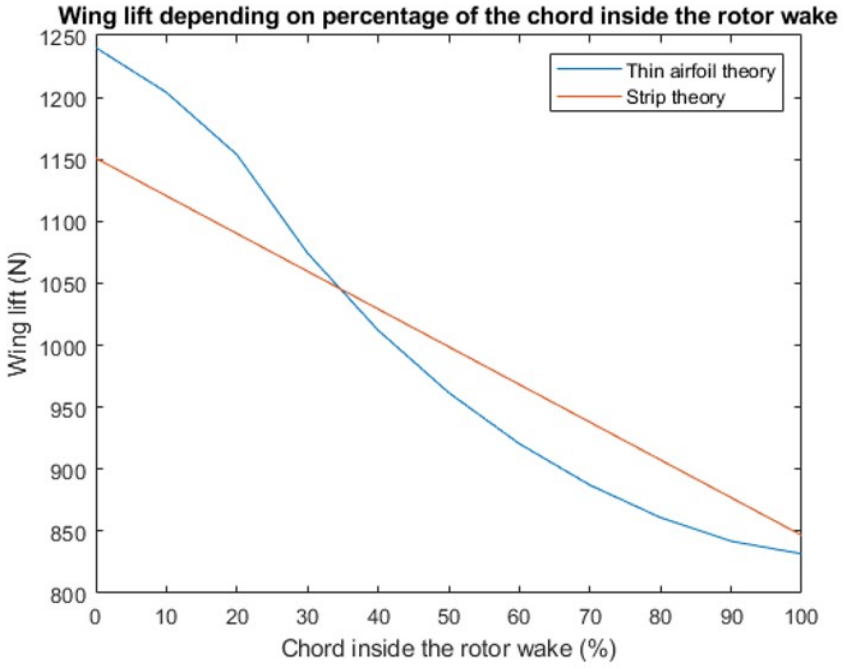

Figure 4.1: Variation of wing lift with the percentage of the root section chord which is inside the rotor wake

From previous studies, it can be checked that wing lift decreases as the wing gets immersed in the rotor wake, due to the increase in the perpendicular component of the velocity that the wing sees, therefore decreasing the angle of attack. From Figure 4.1, it can be seen that the evolution of lift is similar for both theories, although an interpolation method has been used for Strip Theory (as explained in Section 3) and the specific expressions of the theory have been used for Thin Airfoil Theory. These different strategies and the assumption for the Strip Theory are the cause of the highest discrepancies between the results of both theories are found for the cases in which the wing is just partially inside the rotor wake, as can be seen in Table 4.8 and Table 4.9. Because of that, the Thin Airfoil Theory results can be considered more exact for these situations.

One of the main disadvantages of Thin Airfoil Theory is that it can not be used for airfoils with high thickness under certain angles of attack. To study this aspect in detail and simultaneously verify the code developed for this Thin Airfoil Theory, the wing detailed code has been run to calculate the wing lift for several angles of attack and different constant airfoils (of different thickness), using both theories to compare the results (since Strip Theory is considered valid for all the airfoils). The wing chosen for this study has the following geometrical characteristics: wingspan of 10 m and chord of 1.5 m. The flight velocity is set to 30 m/s. The results can be seen in Table 4.10.

From this analysis, it can be checked that the difference between the results of each theory increases as the airfoil thickness increases, for all the values of the angle of attack. Therefore, is has been checked that the Thin Airfoil Theory becomes invalid for thicker airfoils, as stated in

Table 4.10: Comparison of wing lift results of Thin Airfoil Theory and Strip Theory, for different angles of attack and airfoils

AoA (º)	Airfoil	Wing lift (N)		Difference (%)
		Strip Theory	Thin Airfoil Theory	
2	NACA 0012	1372.1	1347.1	1.9
	NACA 0018	1388.1	1347.1	3.0
	NACA 0022	1375.2	1347.1	2.1
	NACA 0030	1152.9	1347.1	-14.4
	SC 1095	1908.9	1847.4	3.3
6	NACA 0012	4028.5	4041.3	-0.3
	NACA 0018	4100.4	4041.3	1.5
	NACA 0022	4045.7	4041.3	0.1
	NACA 0030	3379.9	4041.3	-16.4
	SC 1095	4690.7	1847.4	3.3
10	NACA 0012	6864.9	6735.5	1.9
	NACA 0018	6594.7	6735.5	-2.1
	NACA 0022	6404.9	6735.5	-4.9
	NACA 0030	5601.5	6735.5	-16.8
	SC 1095	7361.2	7235.8	1.7

Chapter 2. This is something the tool user should take into account when selecting the wing airfoil if Thin Airfoil Theory is going to be used for the calculations.

Another consequence of the interactions between wing and rotor is the pseudo ground effect experimented by the rotor due to the existence of the wing surface just below it, as explained in Chapter 3. This makes the rotor thrust increase and it depends on the proximity between wing and rotor. In order to check the actual effect of this phenomenon, the ratio T_g/T_∞ has been calculated for several values of the vertical distance between rotor and wing and different flight velocities, being T_g the actual rotor thrust (including this pseudo ground effect) and T_∞ the thrust which the rotor would develop without considering this effect. The value of this ratio corrected by considering that not the whole rotor is affected by this effect, but just the part which is exactly above the wing (this is done with an interpolation method, as explained in Chapter 3) is finally shown. The selected wing for the study has a wingspan of 10 m and a chord of 1.5 m; the rotor has a radius of 7.127 m; and the ratio of wing and rotor areas is equal to $A_{wing}/A_{rotor} = 0.094$. The results are shown in Table 4.11. In this table, the obtained value for 15 m/s and 1 m of distance is too high (even when it is corrected with the areas factor), due to both the velocity and the distance between rotor and wing being too low. As explained in Section 3, the value which the code would use for the thrust calculations in this case would be 2, due to the limitation imposed.

As can be deduced from this study, this effect becomes more important as the flight velocity decreases and the distance between the rotor and the wing decreases, as expected. Indeed, this effect becomes negligible for velocities higher than 20 m/s and distances higher than 2 m in the vehicle in study, but it is actually important for lower values of these parameters.

Finally, the whole tool structure has been used to calculate the main rotor power of a real

Table 4.11: Magnitude of pseudo ground effect on rotor thrust for different flight velocities and distances to the wing

Velocity (m/s)	Distance rotor-wing (m)	T_g/T_∞	T_g/T_∞ corrected with areas
15	1	15.8532	2.3962
	2	1.3062	1.0288
20	1	1.8091	1.0666
	2	1.1259	1.0109
30	1	1.1140	1.0091
	2	1.0244	1.0021

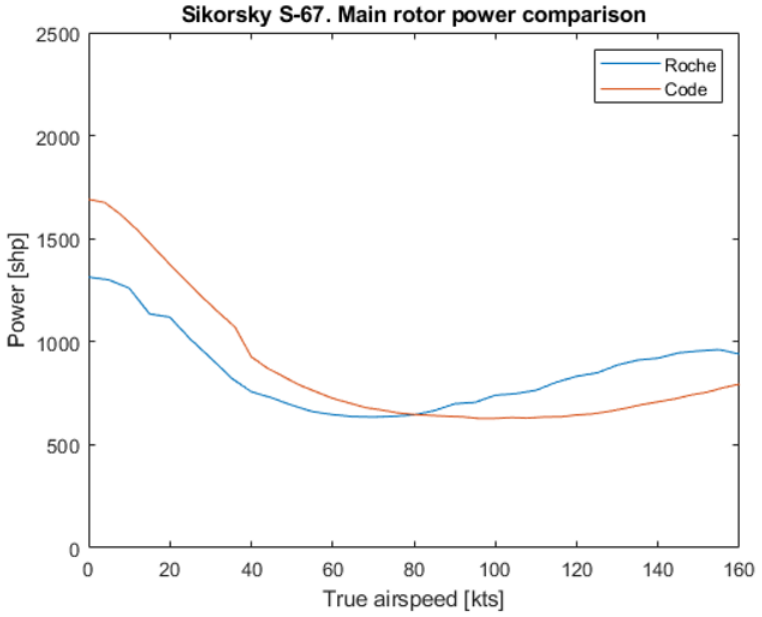

Figure 4.2: Comparison of the rotor power obtained from tool results (red line) with Roche's article data (blue line), as a function of flight speed, of Sikorsky S-67

lift compound helicopter. The helicopter which is going to be used to validate the lift compound helicopter tab of the tools is Sikorsky S-67. A brief description of this helicopter can be found in Chapter 1 and Figure 1.1 illustrates it. The rotor power has been calculated for a range of flight velocities to be compared with the results included in Roche's article [5]. A graphical representation has been made including the evolution of power with flight speed for the tool and Roche's results, and it can be seen in Figure 4.2, where the title *Roche* at the graph's legend corresponds to the data included in Roche's article [5].

In Figure 4.2, it can be seen that the graph obtained from the tool is similar to the one obtained in Roche's article and presents the same evolution, with the power decreasing for values of the flight speed from 0 kt to approximately 50 kts and increasing afterwards. However, it is seen that the tool overpredicts the rotor power for low flight speeds and underpredicts it for high flight speeds, when compared with Roche's data. This is probably due to the fact that the helicopter geometrical properties had to be slightly adapted to be modeled as tool inputs (so they are not exactly equal

to the helicopter real properties). However, errors do not reach 20%.

4.4 Propulsive compound helicopter

To validate and verify the study of propulsive compound helicopters, the codes involved in the analysis of helicopters including a propeller have been run and tested. For running these calculations, the detailed conventional helicopter tool (propulsive compound tab) has been selected, since it contains all the theories and considerations regarding propulsive compound helicopters which have been included in this thesis. Two main studies have been made for this validation and verification. First, the study focuses on the validation of the interaction between the main rotor and the propeller, i.e. how the rotor affects the performance of the propeller (some calculations using both theories and some graphs have been made). Then, the whole code structure has been tested by modeling a real helicopter and comparing the results obtained by the tool with experimental data of this helicopter.

In order to analyse how the contact with the main rotor wake affects the propeller thrust when it is partially inside the wake, the propeller detailed code has been run independently of the rest of the tool codes to manually vary the percentage of the propeller area which is inside the rotor wake. The distance between both elements and the flight velocity have not been changed, but the propeller percentage have been artificially varied. The results of propeller thrust have been represented, as a function of the percentage of the propeller area which is inside the wake, in a graph and it can be seen in Figure 4.3.

From this study, it can be checked that propeller thrust decreases as it gets immersed in the rotor wake, due to the increase in the perpendicular component of the velocity that the blades see, therefore decreasing the angle of attack. Since the propeller thrust does not change so much depending on its percentage inside the wake (just a 5.6% of difference between the situation in which the whole propeller is under the influence of the wake and the situation in which it is totally out of it, in this particular case), it can be concluded that the rotor wake interference is not so relevant in the case of the propeller, for standard distances to the rotor and standard flight velocities. This justifies the method used to simplify the study of propellers partially influenced by the wake, explained in Section 3.1.2.

Finally, the whole tool structure has been used to calculate the main rotor power of a real compound helicopter. The helicopter which is going to be used is Lockheed AH-56 Cheyenne, which is in fact a combined compound helicopter, since it includes a wing and a propeller at its tail. A brief description of this helicopter can be found in Chapter 1 and Figure 1.3 illustrates it. The rotor power has been calculated for a range of flight velocities to be compared with the experimental data included in Johnson's report [18]. A graphical representation has been printed in the same graph where the experimental data is presented, and it can be seen in Figure 4.4.

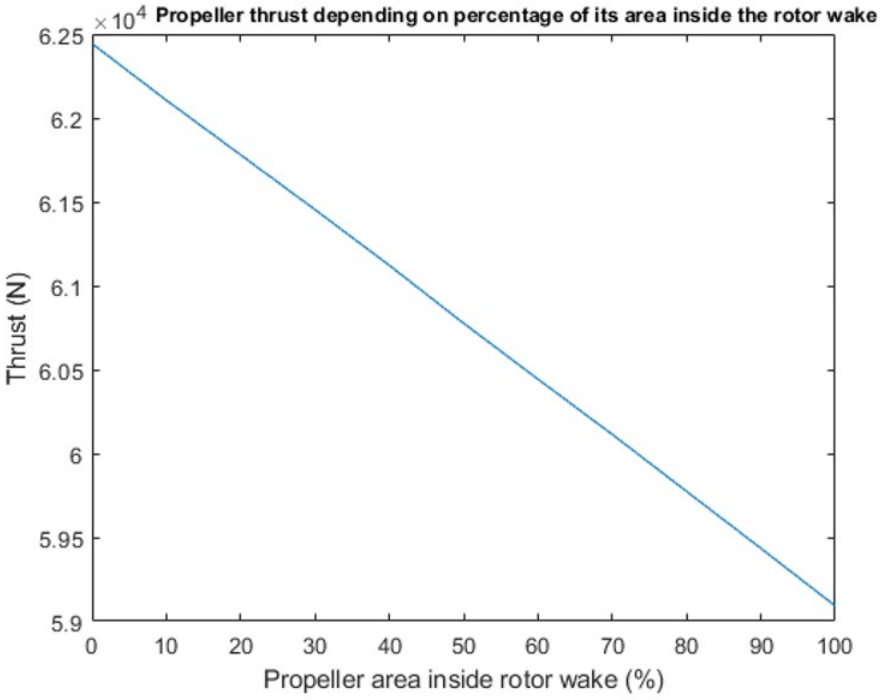

Figure 4.3: Variation of propeller thrust with the percentage of its area which is inside the rotor wake

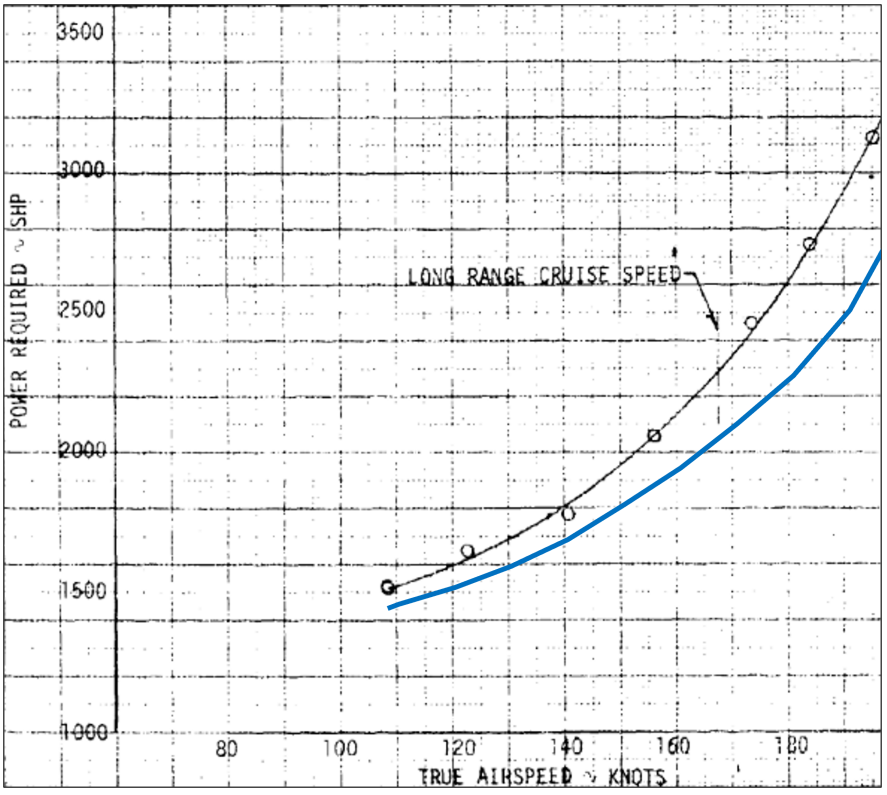

Figure 4.4: Comparison of the evolution of rotor power with flight speed obtained from tool results (blue line) with experimental data (black line) of Lockheed AH-56 Cheyenne. [18, pg. 98]

In Figure 4.4, it can be seen that the graph obtained from the tool is similar to the one obtained with the experimental data and presents the same evolution, with the power increasing from flight velocities equal to 110 kts. However, it is seen that the tool slightly underpredicts the power values, when compared with experimental data included in [18]. This is probably due to the fact that the helicopter geometrical properties had to be slightly adapted to be modeled as tool inputs (so they are not exactly equal to the helicopter real properties) and to the fact that, in experiments, some effects which have not been considered in the tool codes may have affected the results. However, errors do not reach 16%.

After all these studies have been analysed, a good agreement has been found between the different theories and experimental data, which allows the validation and verification of the the wing and propeller codes independently and also the lift, propulsive and combined compound helicopter codes. Therefore, it can be concluded that the methodologies used in this thesis to study compound helicopters are adequate.

5 Case study

5.1 Compound helicopters

In this section, a direct application of the software developed in this thesis will be made. Three of the tools created are going to be used to model twelve different helicopters whose performance will be compared and analysed, under the same conditions. The tools which are going to be used for this analysis are the following ones: detailed conventional helicopter tool (with which a conventional lift, propulsive and combined compound helicopter and a simple conventional helicopter will be modeled), detailed coaxial helicopter tool (with which a coaxial lift, propulsive and combined compound helicopter and a simple coaxial helicopter will be modeled) and basic tandem helicopter tool (with which a tandem lift, propulsive and combined compound helicopter and a simple tandem helicopter will be modeled). The main structure of all these helicopters has a mass of 5000 kg, but the total mass of each of the helicopter in study increases with its complexity, depending on the amount of components (rotors, wings and propellers) they include.

First, the geometrical and aerodynamic parameters which have been selected to make the study are going to be presented. They have been set considering typical values for the characteristics of these types of vehicles.

The flight conditions, which are the same for all the helicopters in the study, are presented in Table 5.1.

Table 5.1: Flight conditions of the case study

Velocity	30 m/s
Trajectory angle	0^o
Altitude	500 m

Now, the properties of the helicopter main rotor are shown in Table 5.2. All the rotors have the same characteristics, including both rotors of coaxial and tandem helicopters.

Table 5.2: Main rotor properties of the case study

Number of blades	4
Radius	7.127 m
Root cut-out	20%
Flapping hinge position	0%
Rotation velocity	280 rpm
Chord distribution	Constant
Chord	0.435 m
Twist distribution	No twist
Pitch angle	0^o
Airfoil distribution	Constant
Airfoil	NACA0012

For the case of the conventional helicopters (the coaxial and tandem helicopters do not have a tail rotor), the properties of the tail rotor are shown in Table 5.3.

Table 5.3: Tail rotor properties of conventional helicopters of the case study

Number of blades	2
Radius	1.349 m
Root cut-out	10%
Flapping hinge position	0%
Rotation velocity	1356 rpm
Chord distribution	Constant
Chord	0.286 m
Twist distribution	No twist
Pitch angle	0^{o}
Airfoil distribution	Constant
Airfoil	NACA0012

The geometrical and aerodynamic properties of the wing of the lift compound helicopters in the study, which are the same for the three helicopter configurations, are presented in Table 5.4.

Table 5.4: Wing properties of the case study

Wingspan	15 m
Chord distribution	Constant
Chord	2 m
Twist distribution	No twist
Pitch angle	5^{o}
Airfoil distribution	Constant
Airfoil	NACA0012
Oswald efficiency	1
Vertical distance rotor-wing	1.5 m
Horizontal distance rotor-wing	0 m
Mass	200 kg
Half wing	No
Rotor induced velocity factor	1.5

Finally, the geometrical and aerodynamic properties of the propeller of the propulsive compound helicopters in the study, which are the same for the three helicopter configurations, are presented in Table 5.5.

After all the geometrical and aerodynamic parameters of the helicopters in study have been defined, they have been introduced in their corresponding tools' tabs and, following the flow described in Chapter 3, the results of main rotors thrust and total vehicle power of each of the twelve vehicles modeled have been obtained. These results are shown in Table 5.6, Table 5.7 and Table 5.8. These tables show the results corresponding to each of the general helicopter configurations (conventional, coaxial and tandem). In the tables, the differences between thrust and power of the compound configurations and thrust and power of their corresponding simple configuration are presented, in percentages.

Table 5.5: Propeller properties of the case study

Number of blades	3
Radius	1.5 m
Root cut-out	5%
Rotation velocity	2000 rpm
Chord distribution	Constant
Chord	0.2 m
Twist distribution	No twist
Blade pitch angle	15^{o}
Airfoil distribution	Constant
Airfoil	NACA0012
Horizontal distance rotor-propeller	3 m
Vertical distance rotor-propeller	0.5 m

Table 5.6: Thrust and power results of the simple and compound conventional helicopters of the case study

Conventional configuration				
Helicopter type	Thrust (N)	Difference (%)	Power (W)	Difference (%)
Simple (no compound)	58619.5	-	512600.1	-
Lift compound	53750.9	-8.3	452976.3	-11.6
Propulsive compound	58527.7	-0.2	514113.3	0.3
Combined compound	53736.5	-8.3	454198.8	-11.4

Table 5.7: Thrust and power results of the simple and compound coaxial helicopters of the case study

Coaxial configuration					
Helicopter type	Rotor	Thrust (N)	Difference (%)	Power (W)	Difference (%)
Simple (no compound)	Top	63502.3	-	559600.2	-
	Bottom	49760.3	-	556000.3	-
Lift compound	Top	60270.5	-5.1	525397.5	-6.1
	Bottom	48121.2	-3.3	525798.7	-5.4
Propulsive compound	Top	63224.1	-0.4	557648.7	-0.4
	Bottom	49919.6	0.3	555987.5	0.0
Combined compound	Top	60670.0	-4.5	528476.3	-5.6
	Bottom	47771.4	-4.0	523428.0	-5.9

Table 5.8: Thrust and power results of the simple and compound tandem helicopters of the case study

Tandem configuration					
Helicopter type	Rotor	Thrust (N)	Difference (%)	Power (W)	Difference (%)
Simple (no compound)	Front	49549.6	-	359600.3	-
	Rear	48566.9	-	361200	-
Lift compound	Front	47299.1	-4.5	345752.6	-3.9
	Rear	46018.0	-5.3	347653.8	-3.8
Propulsive compound	Front	50719.0	2.36	366960.7	2.1
	Rear	49344.8	1.6	367823.9	1.8
Combined compound	Front	46998.7	-5.1	343525.2	-4.5
	Rear	46309.4	-4.7	343843.6	-4.8

Analysing the results of Table 5.6, it can be seen that the addition of a wing in a conventional helicopter clearly improves its performance, highly offloading the main rotor in terms of thrust and power. However, although it slightly improves the helicopter performance in terms of rotor thrust too, the addition of a propeller does not significantly change the results of the simple configuration for these flight conditions. In fact, the power needed by the vehicle is a bit higher than in the simple case, probably due to the propeller power requirements. The combined compound configuration is also a good strategy to improve the performance of this conventional configuration, mainly due to the wing effect.

A similar behaviour is observed in the case of the coaxial configuration (Table 5.7). The wing clearly offloads both rotors and reduces the helicopter power requirements. The propulsive compound configuration does not significantly change the results: it slightly improves the performance of the top rotor, reducing its thrust and power, but increases a bit the thrust of the bottom rotor. The combined compound configuration clearly improves the performance too, even more than the lift compound configuration for the bottom rotor.

Finally, the tandem helicopters also present a similar behaviour (Table 5.8). The lift compound configuration improves the performance of both rotors. The propulsive compound configuration is not beneficial for the helicopter, since thrust and power of both rotors increase. Lastly, the combined compound configuration is the most beneficial, since it decreases the thrust and power requirements of both rotors even more than the lift compound configuration.

As a conclusion, the addition of a wing in a helicopter with these properties and for these flight conditions is clearly a good solution to improve its performance, and the improvement would become greater as the flight velocity increases (since the wing lift would be higher). The benefits of the wing are specially seen for the conventional configuration. The reason for this is the following one: the wing design is the same for the three configurations, so it creates the same lift; the weight of the conventional helicopter is lower than the coaxial and tandem helicopters ones, so the lift of the rotor of the conventional helicopter is also lower; therefore, the wing lift (which is the same for the three configurations) represents a higher part of the total rotor lift in the conventional helicopter, so the wing *help* is more relevant in this case. In the other hand, it is clear that the addition of a wing will increase the total helicopter weight, but it is up to the user to see if it overall benefits the performance and is worth it.

The addition of a propeller does not significantly improve the performance of any of the vehicles in study. One of the reasons for that is the power requirements of the propeller, which must be added to the helicopter total power, as well as the extra weight it adds to the helicopter. The benefits of the propulsive compound configuration may be seen more clearly in other flight and propeller conditions: higher flight velocities and higher propeller rotation speeds. For the flight velocity of this study, the helicopter drag is not high, so the main rotor can generate the

necessary forward thrust to overcome it without being overloaded and therefore not needing the propeller *help*. However, if the velocity increases, the helicopter drag also increases and the forward thrust necessary to overcome it becomes an important part of the main rotor thrust. In this case, the propeller can generate a huge part of that force, significantly offloading the main rotor and improving the helicopter performance. In the other hand, for higher flight velocities, the angles of attack of the propeller blades decrease (because the flight velocity is perpendicular to the propeller plane of rotation), so the rotation speed should increase to keep a good performance.

Finally, the combined compound configuration has approximately the same effect in the helicopter performance than the lift compound configuration for the three cases in study. Therefore, the lift compound helicopter would be the best solution for this case: the addition of just a wing is better than the addition of both a wing and a propeller for similar performance results, since the propeller increases the complexity, weight and power needs of the vehicle.

In order to further analyse the propulsive compound helicopter performance and the efficiency of the addition of a propeller in a helicopter, another case study has been developed, where the conditions have been selected to be suitable for the propulsive compound configuration. Specifically, the flight velocity is much higher than in the previous case (it has been set to 80 m/s), the propeller rotational velocity has been increased to 3400 rpm and the helicopter mass is much lower than in the previous case (it has been set to 1000 kg). The rest of flight conditions and geometrical and aerodynamic properties keep their values with respect to the previous case study. A propulsive compound helicopter in the conventional configuration (just one main rotor, a tail rotor and a propeller) and its results in terms of main rotor thrust and power have been compared with the ones of its corresponding simple configuration (no compound, i.e. the same vehicle but without the propeller). This comparison is presented in Table 5.9.

Table 5.9: Thrust and power results of the simple and propulsive compound conventional helicopters of the second case study

Helicopter type	Thrust (N)	Difference (%)	Power (W)	Difference (%)
Simple (no compound)	10915.6	-	453500.2	-
Propulsive compound	9816.1	-10.1	420988.4	-7.2

As can be seen in Table 5.9, the thrust and power reduction in the main rotor due to the propeller action is significant for these conditions. The improvement of the vehicle that the propeller makes for these conditions is much more relevant than for the previous ones because of the following reasons. First, the flight velocity is much higher, so the horizontal component of the thrust which the vehicle must develop is also much higher; then, the fraction of this horizontal thrust that the propeller can generate is higher, being its *help* to the main rotor more significant. In fact, in this specific case, the propeller generates almost the whole horizontal force the helicopter needs to perform the flight, i.e. the propeller thrust (which is equal to 4468.7 N) is almost equal to the vehicle drag in this flight. Moreover, since the helicopter is lighter, the vertical force that the

helicopter must develop is lower, so the horizontal force (which is the component that the propeller can generate) becomes a more significant part of the total required force.

After these case studies, it can be concluded that the efficiency of the compound helicopters, especially in case of the propulsive compound configuration, depends on the helicopter characteristics and flight conditions, so it is important to deeply analyse the mission and objectives of the vehicle to decide if the addition of a wing and/or a propeller to the helicopter is convenient.

5.2 Cyclocopter

In this subsection, a direct application of the cyclocopter tool is going to be shown. First, the thrust and power of a single cyclocopter rotor in forward flight will be calculated using both sinusoidal pitch variation theory and four-bar linkage variation mechanism system theory. Then, a whole cyclocopter with four rotors will be analysed to calculate the thrust that each of its rotors must develop under certain forward flight conditions.

First, the characteristics chosen for the single rotor are presented in Table 5.10.

Table 5.10: Single rotor properties of the cyclocopter case study

Number of blades	4
Radius	0.3 m
Blade span	0.4
Rotation velocity	1000 rpm
Chord	0.2 m

The flight conditions selected for this study are shown in Table 5.11.

Table 5.11: Flight conditions for the cyclocopter single rotor case study

Altitude	30 m
Horizontal velocity	10 m/s
Vertical velocity	2 m/s

Besides the previous parameters, the necessary inputs of the sinusoidal pitch variation theory have been set and they are presented in Table 5.12.

Table 5.12: Sinusoidal pitch variation theory inputs for the cyclocopter single rotor case study

Pitch amplitude	20^{o}
Maximum pitch angle	20^{o}

And the necessary inputs of the four-bar linkage mechanism system theory are shown in Table 5.13.

After introducing these numbers in the corresponding fields of the second tab of the cyclocopter tool and pressing both *Calculate* buttons, the results of thrust and power obtained using both

Table 5.13: Four-bar linkage mechanism system theory inputs for the cyclocopter single rotor case study

L2	0.0065 m
L3	0.3015 m
L4	0.0110 m
Phase angle of eccentricity	5^{o}
Maximum pitch angle	20^{o}

theories are presented in Table 5.14.

Table 5.14: Results of thrust and power for the cyclocopter single rotor case study

Theory	Thrust (N)	Power (W)
Sinusoidal pitch variation	8.3	38095.6
Four-bar linkage mechanism system	12.6	25201.2

The second case study focuses in a whole cyclocopter. The geometrical properties for each of its rotors and the flight conditions are the same as in the single rotor study previously presented. For this study, some extra inputs must be introduced and their chosen values are presented in Table 5.15.

Table 5.15: Inputs for the whole cyclocopter case study

Number of rotors	4
Weight	6 kg
Flat plate area	2 m^2
Bottom limit of pitch amplitude	0^{o}
Top limit of pitch amplitude	60^{o}
Thrust convergence tolerance	0.5 N

After introducing these numbers in the corresponding fields of the third tab of the cyclocopter tool and pressing the *Calculate* button on the right, the tool shows the following results: the thrust that each of the four rotors must develop for performing this flight is equal to 34.6 N and it is achieved with a sinusoidal pitch variation of amplitude equal to 5^{o}.

6 Conclusions

6.1 Achievements

The main objective of this work is the further development of a rotary-wing preliminary design tool, by adding new functionalities which complement the tool and widen its scope and possibilities. In this regard, the main contribution of this thesis is the inclusion of the study of compound helicopters performance, which materializes in the addition of three new tabs to each of the helicopters specific tools. Furthermore, a new specific tool has been created to address a new kind of rotary-wing vehicle, the cyclocopter. Moreover, some new characteristics have been included in the previous codes (the ones which analyse no-compound helicopters), such as the addition of the ground effect to the rotors study. These developments have represented a relevant improvement in terms of tool complexity, have broadened its possibilities and increased the depth of the study it develops.

The tools developed in this thesis should be used for the preliminary design of rotary-wing vehicles, since they are useful to get a first approximation of the performance of the vehicle in design. However, they also have some limitations, so they should not be used as the definitive tools to base on for developing a complete design. To make a deeper and more detailed design of the vehicle, more complex tools should be used, such as finite elements applications or computational fluid mechanics programs. The tools in this thesis are useful to get a good starting point on which to base the next stages of the vehicle design.

The studies presented in Chapter 4 demonstrate that the tools can provide reliable results for all the vehicles configurations they address. The obtained results are very similar to the ones obtained by similar tools and real experimental data. Although some differences are found in these comparisons, the error and difference percentages can be considered small enough for the purpose of the tools, so they are an efficient starting point and develop a reliable preliminary design.

After analysing the compound helicopters performance results obtained, it can be concluded that the addition of a wing (making a lift compound helicopter) improves the helicopter performance in flight conditions implying high forward velocities, but its efficiency decreases as flight speeds decrease or the helicopter goes into axial flight. A more careful study must be done to analyse the efficiency of a propeller, since a trade-off between its help to the main rotor propulsion and the additional power it requires must be reached. Additionally, its efficiency highly depends on the helicopter characteristics and flight conditions.

One of the main advantages of the tools developed is their possibility to quickly determine the feasibility of whatever rotary-wing vehicle solution the user thinks of, as well as the possibility of comparing some different designs in order to determine which one is more efficient or matches the user interests. As demonstrated in Chapter 5, this is done in a quick and visual manner, since

not many parameters are necessary to perform the study and they are introduced in the different tabs in a very intuitive way. The reliability, versatility and open-source nature of these tools make them attractive for students' analysis and people interested in developing the first stages of larger design projects.

6.2 Further work

One of the main advantages of the versatility of the tools developed in this thesis is the possibility of integrating many new aspects to make their study deeper, more detailed and more accurate (actually, that is the main objective of this thesis). Therefore, wide further works may be developed to complete these tools.

With respect to the wing study, the further work possibilities focus on the analysis of the aerodynamic interactions between the main rotor wake and the wing. For instance, the application of more specific theories, such as Vortex Theory, to model the wake behaviour would be interesting. For the case of the propeller, the possibility of including multiple propellers in the helicopter (such as propellers installed on the wings) could be implemented to model new vehicles configurations. The most interesting aspects to be included in the tools in terms of compound helicopters analysis are related to the interactions between all the elements of the vehicle, such as the effects that the wing and the propeller have in the performance of the other one in combined compound helicopters.

Multiple ideas are also feasible to create new tabs in the existing tools, addressing new study fields. Structural studies would complement the tools very well; for instance, a tab which proposes structural solutions for the helicopter fuselage based on the vehicle characteristics and mission. Moreover, aerodynamic moments could be also taken into account to implement control laws for both helicopters and drones. Finally, a section for gas turbines studies may also be added to analyse powerplants performance and efficiency, which is one of the most important topics in current aeronautical engineering.

References

[1] Tomás Fontes, *Conceptual Design and Performance Analysis Tool for Rotorcraft Systems*, Masters' Thesis, Instituto Superior Técnico, Lisbon, 2020.

[2] Alberto Ramos, *Analysis and description of cyclocopter performances*, Masters' Thesis, Instituto Superior Técnico, Lisbon, 2021.

[3] Robert A. Ormiston, *Revitalizing Advanced Rotorcraft Research—and the Compound Helicopter: 35th AHS Alexander A. Nikolsky Honorary Lecture*, Journal of the American Helicopter Society, Vol. 61, Iss. 1, 2016, pp. 1-23 (23).

[4] Kevin M. Ferguson, *Towards a Better Understanding of the Flight Mechanics of Compound Helicopter Configurations*, PhD Thesis, University of Glasgow, Glasgow, 2015.

[5] Julian Roche, *Aerodynamic Trade Study of Compound Helicopter Concepts*, Masters's Thesis, Embry-Riddle Aeronautical University, Daytona Beach, 2015.

[6] J. Gordon Leishman, *Principles of Helicopter Aerodynamics*, Cambridge Aerospace Series, Cambridge, 2006.

[7] *XFLR5: Analysis of foils and wings operating at low Reynolds numbers*, Purdue University, West Lafayette, 2009.

[8] J. Nedic, B. Ganapathisubramani, J. C. Vassilicos, *Drag and near wake characteristics of flat plates normal to the flow with fractal edge geometries*, Imperial College of London, London, 2013.

[9] Ahmad Faiz Aiman Faisal, Aslam Abdullah, Sofian Mohd., Mohammad Zulafif Rahim, Bambang Basuno, *Classifying NACA airfoils based on Thin Airfoil Theory*, ARPN Journal of Engineering and Applied Sciences, Vol. 14, Iss. 11, 2019, pp. 2087–2093 (7).

[10] Charles R. O'Neill, *Thin Airfoil Theory*, Oklahoma State University, Stillwater, 2000.

[11] Brian Cantwell, *AA 200A Applied Aerodynamics. Chapter 12: Wings of finite span*, Class Lecture, Stanford University, Stanford, 2014.

[12] Martin O. L. Hansen, *Aerodyamics of wind turbines*, 2008.

[13] I. C. Cheeseman, W. E. Bennett, *The Effect of the Helicopter Rotor Ground on a Helicopter Rotor in Forward Flight*, Aeronautical Research Council, London, 1955.

[14] Fredric H. Schmitz, *Reduction of Blade-Vortex Interaction (BVI) noise through X-force control*, Journal of the American Helicopter Society, Vol. 43, Iss. 1, 1998, pp. 14-24 (11).

[15] André Bauknecht, Xing Wang, Jan-Arun Faust, Inderjit Chopra, *Wind Tunnel Test of a Rotorcraft with Lift Compounding*, Journal of the American Helicopter Society, Vol. 66, Iss. 1, 2021, pp. 1-16 (16).

[16] João Morgado, *JBLADE v17 Tutorial*, Universidade da Beira Interior, Covilhã, 2013.

[17] UIUC Propeller Database - Volume 1. URL: https://https://m-selig.ae.illinois.edu/props/volume-1/propDB-volume-1.html. Retrieved: 07/2021.

[18] John N. Johnson, et al, *Attack helicopter evaluation AH-56A Cheyenne compound helicopter*, Army Aviation Systems Test Activity Edwards Air Force Base, California, 1972.

[19] Bing-Chen Wang, *MECH 3492 Fluid Mechanics and Applications. Chapter 4: Inmersed Body Flow*, Class Lecture, University of Manitoba, Winnipeg, 2017.

[20] Kevin Ferguson, Douglas Thomson, *Flight Dynamics Investigation of Compound Helicopter Configurations*, Journal of Aircraft, Vol. 52, Iss. 1, 2015, pp. 156–167 (12).

[21] G. Sriram, Puneet Singh, *Multi-mission aircraft RC2 Reconfigurable Compound Rotor Craft*, Indian Institute of Techonology, Kanpur, 2011.

[22] David Marten, Juliane Wendler, *QBlade Guidelines*, 2013.

[23] David Biermann, Edwin P. Hartman, *The aerodynamic characteristics of six full-scale propellers having different airfoil sections*, Langley Memorial Aeronautical Laboratory, McLean, 1939.

[24] Miguel Cabeleira dos Santos, *Analytical Model for the Performance Curves of a Family of Propellers based on Wind Tunnel Tests*, Masters' Thesis, Universidade da Beira Interior, Covilhã, 2018.